THE KINETICS OF ENDOSOME PROCESSING

Thesis presented by

SEETSELA LEGALATLADI

in fulfilment of the requirements for the degree of

MASTER OF SCIENCE

in

MEDICAL SCIENCES (MEDICAL BIOCHEMISTRY)

in the

FACULTY OF MEDICINE

UNIVERSITY OF CAPE TOWN

SUPERVISOR: Associate Professor Lutz Thilo

October 1994

ABSTRACT

Cells take up extracellular material by means of a constitutive process known as endocytosis. During endocytosis, plasma membrane invaginates and pinches off to form intracellular vesicles. These subsequently interact amongst themselves and become part of a complex system of peripheral tubulo-vesicular structures which constitute early endosomes and from where recycling of internalised plasma membrane mainly occurs. Subsequently, endocytic contents can be seen in morphologically distinct multi-vesicular bodies (MVB) or late endosomes, until it is transferred finally to secondary lysosomes, where degradation takes place.

A major question concerning the mechanisms(s) of endosome processing, is whether it operates by means of a randomised compartment, where internalised membrane and contents are pooled, or by way of a time-structured organelle through which membrane and contents move in a sequential manner to their different destinations.

With regard to the structural nature of endosomes, two models are presently under consideration: The maturation model, where there is a gradual transformation of early endosome to late endosomes. This occurs by continuous addition of new membranes from intracellular sources and removal of cell surface-derived membranes for recycling. The other model is the vesicular traffic model, where early and late endosomes exist as distinct compartments, with transfer of endocytic contents (and

membrane?) occurring by means of vesicular traffic between them.

The present thesis looks at the behaviour of internalised cell surface-derived membrane marker in comparison with the behaviour of endocytosed HRP (horse-radish peroxidase) as a fluid-phase contents marker. The pooling and/or segregation in the endosome was measured by determining co-localization with HRP. Co-localization of the two markers in the endosome is studied by using the ability of HRP to catalyse the crosslinking of membrane marker in endosomes with DAB (3,3'-diaminobenzidine), rendering the membrane marker detergent insoluble.

To study the kinetic behaviour of membrane marker, radioactive galactose was covalently bound to cell-surface glycoconjugates on mouse macrophage-cells, $P388D_1$, as catalysed by galactosyltransferase. This provided a general membrane marker. After endocytosis-derived redistribution of membrane marker between the cell surface and endosomal membrane, a steady state was established with about 16% of the label on internal membranes. The bulk of the label on the cell surface was removable by subsequent treatment with ß-galactosidase.

Two major experimental scenarios were used to compare the kinetic behaviour of membrane marker and contents marker. In the first scenario, membrane was allowed to redistribute to steady state, i.e. until membrane traffic did not cause any further redistribution of label between plasma membrane and endosomes. This was followed by endocytic uptake of HRP into

endosome, or displacement of HRP out of the endosome compartment. The degree of detergent solubility of membrane marker was monitored for different times during the process. In the second scenario, the endosome compartment was first filled with HRP, followed by internalisation of membrane marker while HRP was chased out of the endosome compartment.

In the first scenario, the sequential behaviour of the endosome contents marker, HRP, was shown by immediate gradual decline, or increase, in detergent solubility of the membrane marker during endocytic uptake, or displacement of HRP out of endosome, respectively.

In the second experimental scenario, randomised behaviour of membrane marker was observed by a gradual decline in detergent solubility due to accumulation of membrane marker intracellularly with first-order kinetics. This continued while HRP gradually moved out of the endosome compartment, which led to the detergent solubility of the membrane marker rising again.

The results of this work indicated that the contents marker, HRP, was processed in a sequential manner. In contrast, the membrane marker was processed in a random fashion. Random processing of membrane was lost for endocytosis at lower temperatures.

ACKNOWLEDGEMENTS

I would like to thank the following:

- My supervisor, Prof. Lutz Thilo, for his patience, excellent supervision and support.

- My family, for their encouragement and moral support throughout this study.

- The technical staff in the department, including the tissueculture laboratory. Especially Dr Tommy Haylett and Steve Fortuin for being always available to offer assistance whenever necessary.

- Mrs Rose Marie Estment for the typing of this manuscript.

- For financial support: The UCT Postgraduate Scholarships Office, the DAAD (Deutscher Akademischer Austauschdienst), the FRD (Foundation for Research and Development), and the Department of Medical Biochemistry, especially Prof. Wieland Gevers.

ABBREVIATIONS AND SYMBOLS

BSA	= Bovine serum albumin
FCS	= Foetal calf serum
EDTA	= Ethylene diamine tetracetic acid
Hepes	= N-2-hydroxyethyl piperazine-N'-2'-ethane sulphonic acid
Thimerosal	= Ethylmecurithiosalicylic acid (Na+ salt)
HRP	= Horse Radish Peroxidase
SDS	= Sodium dodecyl sulphate
DAB	= 3,3' Diaminobenzidine
ßgal	= ß-galactosidase
^{3}H-UDP-Gal	= Tritiated uridine-diphosphogalactose
^{14}C-UDP-Gal	= ^{14}C-labelled uridine-diphosphogalactose
rpm	= Revolutions per minute
g	= Acceleration due to gravity
dpm	= Disintegrations per minute
°C	= Degree Celsius
PNS	= Postnuclear supernatant
Ci	= Curie
DNAse	= Deoxyribonucleic acidase

CONTENTS

LIST OF FIGURES

CHAPTER 1

INTRODUCTION

1.1 The process of endocytosis

Endocytosis is a constitutive process by which cells take up extracellular material (1,2,3,4). A distinction may be made between the uptake of large particles, phagocytosis, and of solutes and fluids, fluid-phase pinocytosis, or receptor-mediated uptake. Receptor-mediated uptake involves the specific binding with high affinity of soluble ligand molecules to receptor molecules on the cell surface membranes. During endocytosis, the plasma membrane invaginates, and pinches off, to form intracellular vesicles which subsequently interact amongst themselves and with other intracellular membranes (Fig. 1.1). Elements of the cytoskeleton such as actin, microtubules and intermediate filaments play a role in endocytosis (5,6,7).

Both fluid-phase uptake and receptor-mediated uptake are mediated by coated pits, which then form coated vesicles. The "coating" is a morphological feature apparent in electron micrographs (8,9), due to the presence of a lattice made from non-globular protein called clathrin (10), which underlies the invaginated patches of plasma membrane (coated pits). Not all fluid phase is mediated by coated pits as non-coated vesicles may also be involved. Selective inhibition also occurs, for example, receptor-mediated uptake is inhibited by low $[K^+]$ or hypertonic medium whilst fluid phase uptake is not (3a).

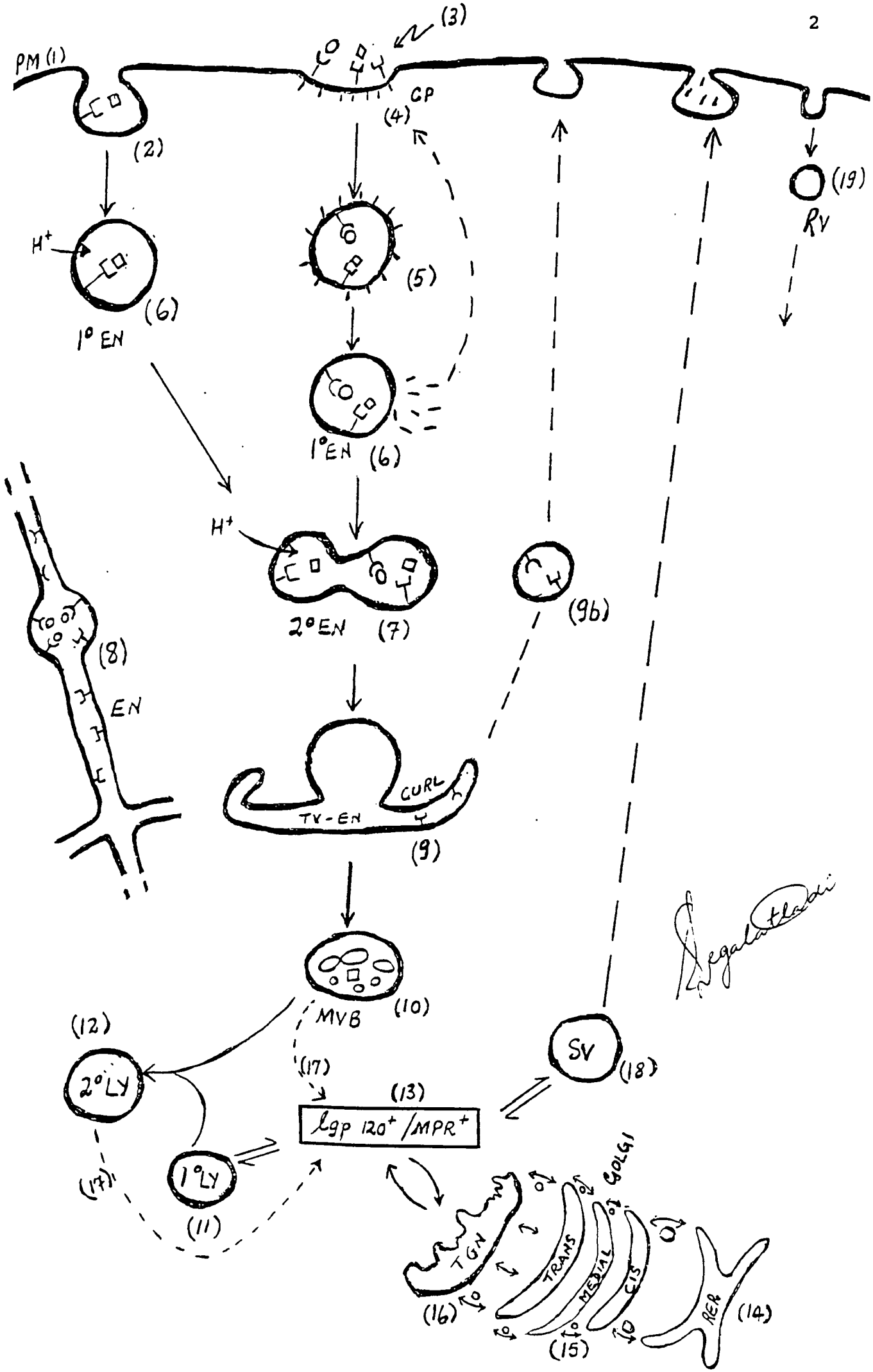
PM (1)
(2)
(3)
CP
(4)
(5)
(6)
1° EN
H+
(19)
RV
1°EN (6)
2°EN (7)
(8)
EN
TV-EN
CURL
(9)
(9b)
MVB (10)
(11)
1°LY
(12)
2°LY
(13)
lgp 120+ /MPR+
(14)
RER
(15)
(16)
TGN
TRANS
MEDIAL
CIS
GOLGI
(17)
(18)
SV

Fig. 1.1: Schematic view of membrane traffic between the intracellular vacuoles and plasma membrane.

(1) PM, plasma membrane. (2) Non-coated pit. (3) Receptor-ligand complexes, clustering in coated pit. (4) CP, coated pit. (5) Coated vesicle. (6) 1°EN, primary endosome, uncoating, with clathrin coat recycling to the plasma membrane. (7) 2°EN, secondary endosome, intra-endosomal acidification leads to dissociation of receptor-ligand complex. (8) Tubular endosome. (9) TV-EN, tubular-vesicular endosome; CURL, compartment for uncoupling of receptor and ligand. (9b) Recycling vesicle with receptors. (10) MVB, multi-vesicular body. (11) 1°LY, Primary lysosome. (12) 2°LY, secondary lysosome. (13) $lgp120^{+}/MPR^{+}$ compartment, interaction point between endocytic and secretory/biosynthetic pathways. (14) RER, rough endoplasmic reticulum. (15) Golgi Apparatus. (16) TGN, trans-Golgi network. (17) Possible pathway of communication between endocytic membranes and secretory and biosynthetic compartments. (18) SV, secretory vesicle. (19) RV, Retrieval of secretory membrane (retrieval vesicle).

Endocytic vesicles become part of a complex system of peripheral tubulo-vesicular structures which constitute the early endosome compartment. Subsequently endocytic contents can be seen in morphologically distinct multi-vesicular bodies (MVB), until it is commonly transferred to secondary lysosomes, where degradation occurs.

1.2 Membrane compartments along the endocytic pathway (cf. Fig. 1.1).

Endosomes can be classified into early endosomes and late endosomes which are functionally and compositionally distinct (11-13). Early endosomes, which correspond to a network of tubular and tubulovesicular structures communicate mainly with the plasma membrane. Extended tubular networks have also been seen *in vivo* (14).

Acidification of the endosome lumen starts immediately after internalisation, and it is the low pH (5.0 - 6.2) which results in dissociation of receptor-ligand complexes in the tubular part, CURL (compartment of uncoupling of receptor and ligand) of this tubular-vesicular endosome (15,16). The early endosome is the major sorting station from where most receptors are recycled back to the plasma membrane, within less than about 5 minutes after internalisation. *In vitro* studies suggest that early endosomal vesicles are highly fusogenic amongst each other, but lose this property with a half-life of minutes (17-22).

After internalisation, endocytic contents are seen in late

endosomes within 15 minutes, and in vitro studies suggest that late endosomes are less fusogenic (17-20). The late endosomes, morphologically distinct as multivesicular bodies (MVB), communicate mainly with the last pre-lysosomal compartment, lgp120^{+}/MPR^{+} (lysosomal glycoprotein 120/mannose-6-phosphate receptor).

Lysosomes are morphologically heterogenous organelles, and this is attributable in part to the fact that they represent various stages in a dynamic process of intracellular digestion (22a). The composition of lysosomal membranes is very distinct from that of the endosomes and plasma membrane (13,24). Primary lysosomes are small granules, with relatively homogeneous content, not yet involved in digestive events. Larger bodies with heterogeneous content are called secondary lysosomes, and are believed to result from fusion of primary lysosomes with endocytic vacuoles (MVB) (23).

Further acidification occurs in the secondary lysosomes, the main site of degradation. Secondary lysosomes can be isolated from the endosomes on the basis of their higher density (15,16). In vivo studies suggest that there is little transfer of membrane occurring during endosome to lysosome transfer of endocytic contents (24).

1.3 Relationship between endocytic and secretory pathways (Fig. 1.1)

The secretory pathway consists of the endoplasmic reticulum, where biosynthesis of proteins occurs, followed by glycosylation and sorting of protein in the Golgi Apparatus (25). The sorting process distinguishes proteins scheduled for constitutive secretion from those which are directed to lysosomes or those which are stored in secretory granules, until secretion occurs upon appropriate stimulation.

The lysosomal enzymes share a common pathway with secretory proteins and membrane proteins during early stages of biosynthesis, until they are sorted out and targeted by membrane associated mannose-6-phosphate receptors (MPR) (26,27). A compartment, which is positive for both lysosomal glycoprotein of MW 120kD and mannose phosphate receptor ($lgp120^+/MPR^+$) and is more acidic than trans-Golgi network (TGN) has been established as the last obligatory pre-lysosomal compartment of the endocytic pathway, and as the site of interaction with the secretory pathway (28).

The $lpg120^+/MPR^+$ compartment is thus common to both the endo- and exocytic pathways. Retrieval of secretory granule membrane after secretion is a process independent of endocytosis (29), and its pathway leads extensively through the trans-Golgi cisternae, probably also via the $lgp120^+/MPR^+$ compartment.

Recycling of cell surface glycoproteins through trans-Golgi compartments has been reported, as observed via resialylation of these glycoproteins after removal of sialic acid residues at the cell surfaces (30,31).

1.4 Structural nature of endosomes

Transfer of endocytic contents along the different membrane compartments of the endocytic pathway requires inter- and intra-compartmental interaction. Therefore, the question arises concerning the structural development between early and late endosomes. Two models are at present under consideration (Fig.1. 2).

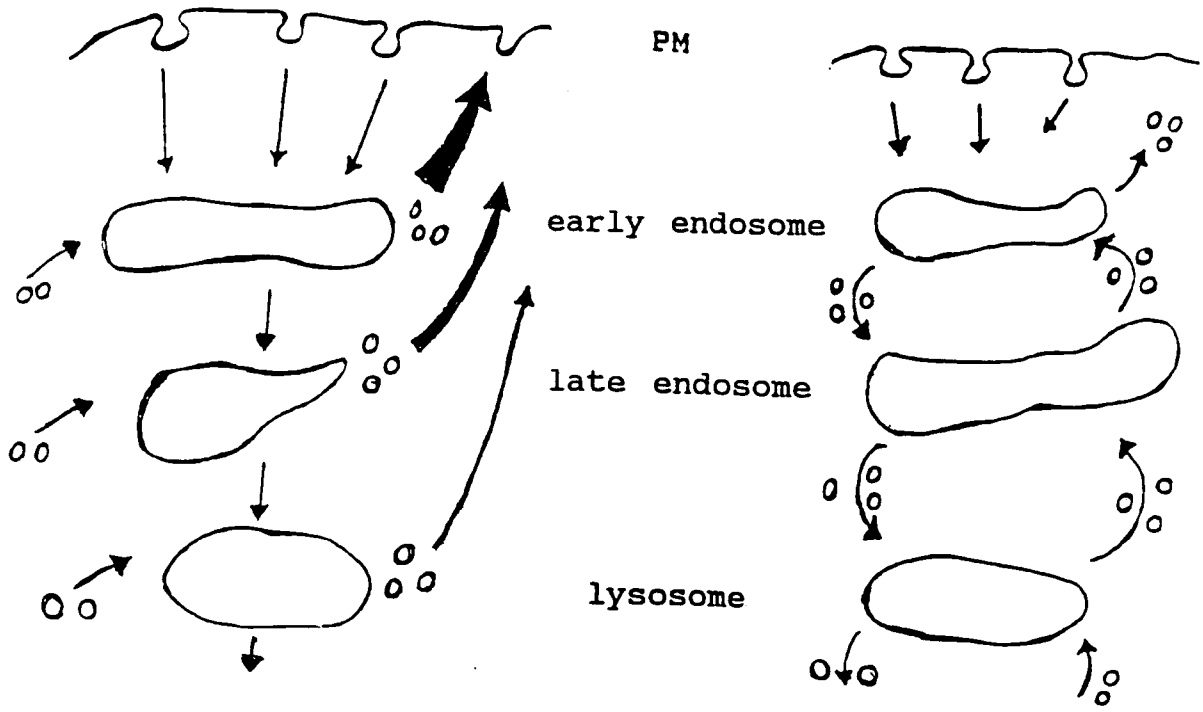

MATURATION MODEL (A) VESICULAR TRAFFIC (B)

Fig. 1.2: Schematic illustration of the concepts underlying the two proposed structural models of endosomes.

In the maturation model (Fig. 1.2A), there is a gradual transformation of an early endosome to a late endosome. There is a continuous addition of new membranes from intracellular sources and removal of cell surface derived membranes for recycling. This leads to a gradual change in membrane composition and in physical properties, both finally resembling those of secondary lysosomes (31a). In the vesicular traffic model (Fig. 1.2B), early and late endosomes exist as distinct compartments, with transfer of endocytic contents occurring by means of vesicular traffic between them (32). Sorting and/or recycling is required at each site of vesicle formation. Late endosomes are also in vesicular communication with secondary lysosomes, most likely via the $lgp120^+/MPR^+$ compartment (28).

Because the maturation model suggests the existence of intermediates between early and late endosomes, it should be possible to detect these experimentally. In some studies, the existence of intermediate structures compatible with maturation have been reported (33,34). In other studies, though, no intermediates were found (12,13). The explanation are that these intermediate structures may be very labile and collapse during cell fractionation.

1.5 Kinetic nature of endosomes

The processing of endocytic contents and endocytic membranes along the pathway can either be sequential or random (Fig. 1.3). These kinetic considerations for endosome processing are not

directly to be associated with one of the above structural models.

In a sequential model, the endosome is perceived as a time-structured organelle, through which membrane and contents move in a sequential manner to their different destinations, i.e. transfer and recycling operate on a first come, first-served basis. According to the random model internalised membrane and contents are pooled, randomised, followed by transfer and recycling based on chance.

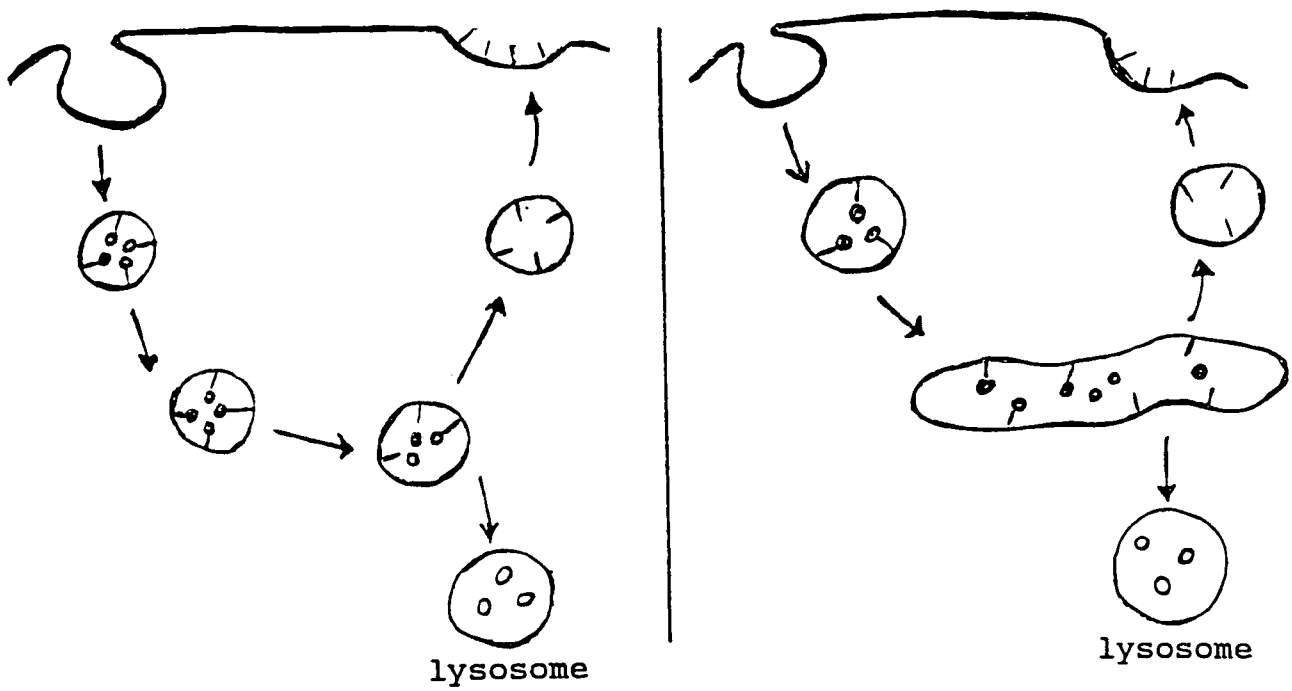

SEQUENTIAL (A) RANDOM (B)

Fig. 1.3. Models showing the kinetics of endosome processing. In Model A endosomal contents are processed in a sequential manner. Model B illustrates how internalized receptor-ligands are segregated and randomised in a common pool. The arrows can operate in either of the structural ways which were indicated in Fig. 1.2.

In HeLa cells, membrane bound receptors for transferrin seem to move through the endosome compartment in a sequential manner (35). Endocytic vesicles which are formed at different times do not intermingle their contents. In contrast, endocytic contents in fibroblast cells appear to become mixed after sequential uptake, as judged by intravacuolar quenching of the first marker, fluorescein dextran, by a second marker, anti-fluorescein antibody, with the latter administered after a lag of 2-5 minutes (36).

In addition, Ward et al (21), using α2-macroglobulin as a labelled ligand that moves towards secondary lysosomes, and introducing a second fluid-phase marker, observed an increase in itermingling of endocytic contents in a late endocytic/ prelysosomal compartment.

1.6 Relation between structural and kinetic considerations of endosomes

On a time scale which is large compared to the time of formation of individual maturing endosomes, lack of communication between them will lead to processing kinetics of a sequential nature. On the other hand, when considered on a time scale which is small in comparison to the time of formation of individual maturing endosomes, there may be randomisation within each maturing endosome. The vesicular traffic model suggests no *a priori* preference for either of the kinetic models.

1.7 The present approach to study the kinetic behaviour of endocytic membrane marker in comparison to contents marker

In order to analyse the kinetic nature of endosomes, the present thesis looks at the behaviour of internalised cell surface-derived membrane marker in comparison with the behaviour of endocytosed HRP as a fluid-phase marker. Co-localization of membrane marker and contents marker (HRP) in endosomes is then studied by using the ability of HRP to catalyse the crosslinking of the membrane marker in endosomes with DAB (3,3' diaminobenzidine), rendering the marker detergent insoluble. The present approach is therefore very similar to the one of Ajioka and Kaplan (35,37), with the difference being that a large number of labelled membrane constituents are observed rather than ligand bound to a single receptor type. Furthermore, DAB crosslinking was also done in intact cells rather than in isolated endosomes in order to avoid losses while doing quantitative analyses.

To provide a general membrane marker, cell-surface glycoconjugates were labelled by covalently binding radioactive galactose to carbohydrate moieties as shown below (38).

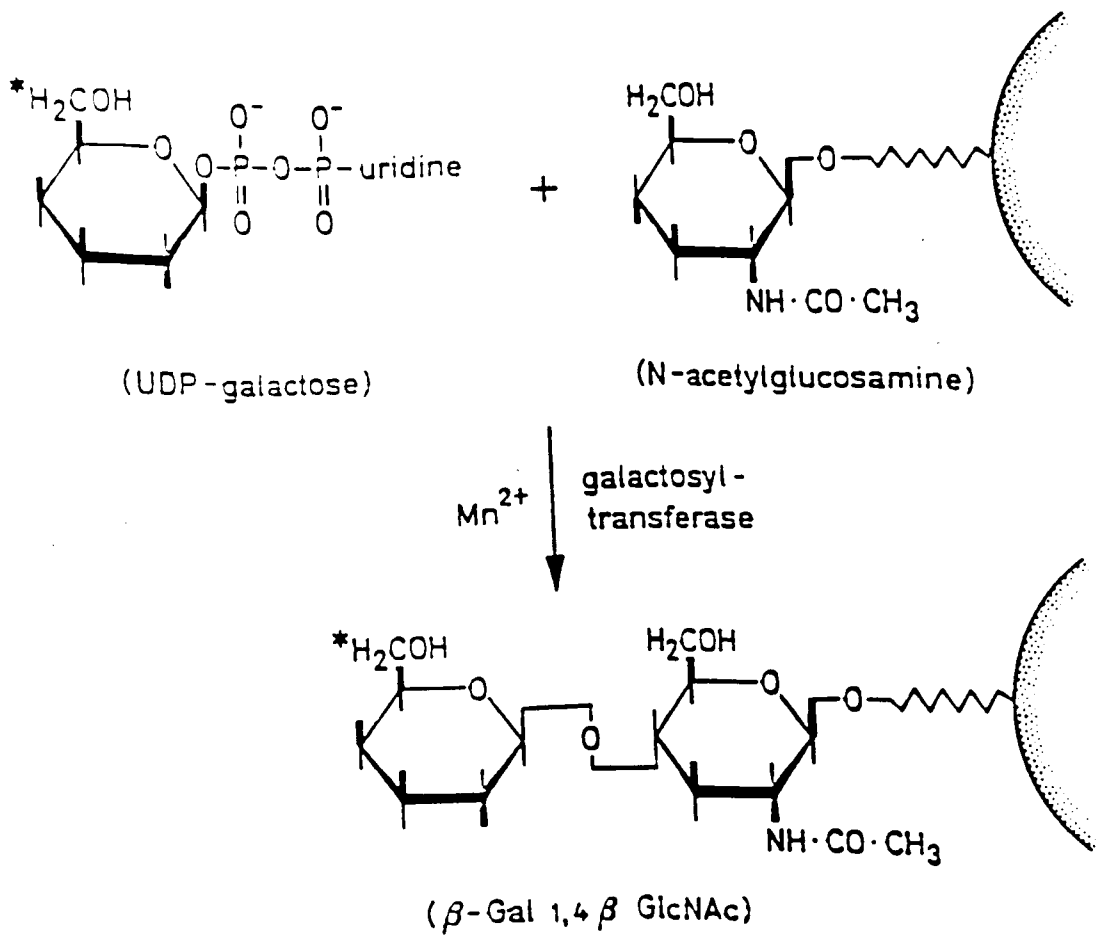

This method labelled membrane constituents of many different molecular sizes between 200-20 Kd (24). In order to label as many different membrane constituents as possible, terminal N-acetylglucosamine moieties on the cell surface were exposed by pretreatment with neuraminidase and ß-galactosidase.

The label has previously been found to behave as a stable and representative membrane marker. It is internalised into intracellular compartments, is recycled to the cell surface, and as a result equilibrates to reach a steady-state distribution between the plasma membrane, endosomes and lysosomes (24,38).

The DAB crosslinking-reaction, first used by Courtoy et al. (39), caused a density shift of endosomes containing HRP. DAB is selectively oxidised in the presence of peroxide (H_2O_2) and

trapped as a dense compound as seen by electron microscopy in particles containing HRP. The associated membrane proteins are rendered detergent insoluble.

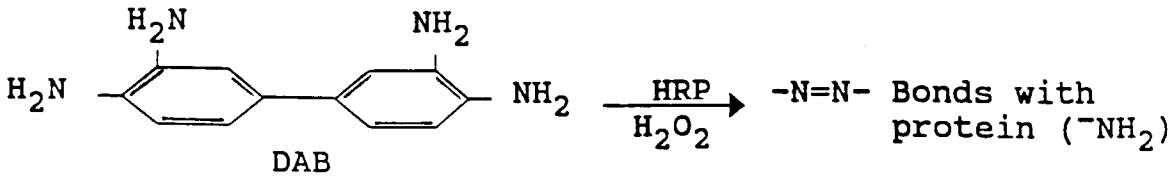

This reaction allows one to measure the co-localization of HRP with an endocytic marker (ligand or membrane marker) in the vesicle.

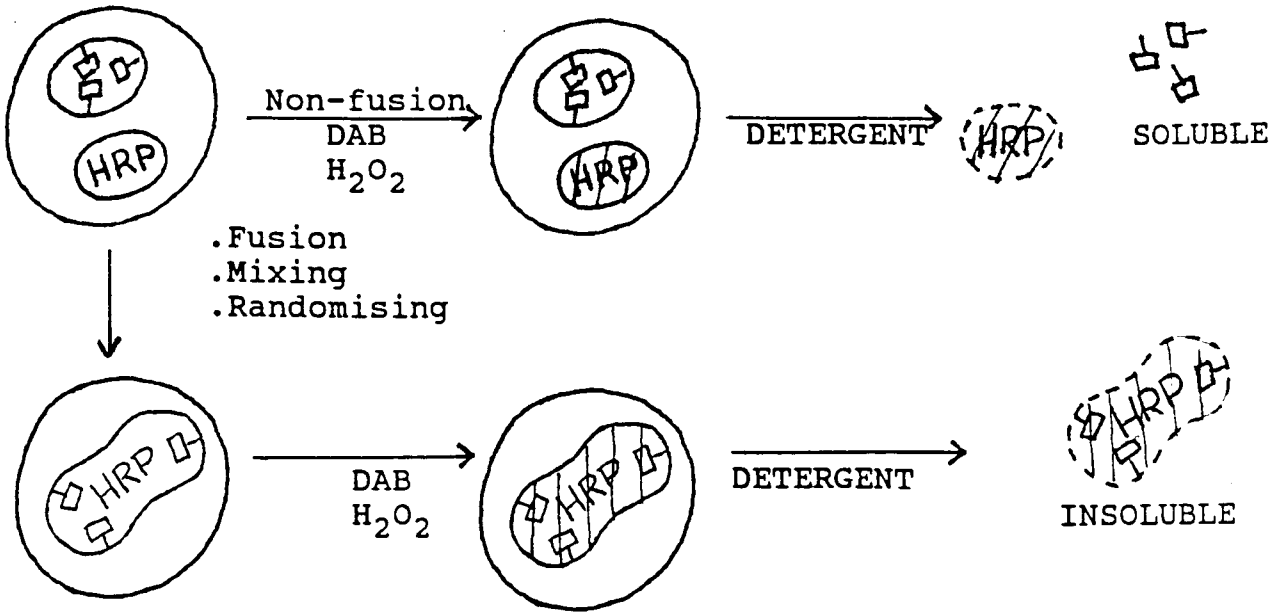

1.8 Scenario for kinetic analyses

Various experimental scenarios can be devised to compare the kinetic behaviours of the membrane marker and the contents marker.

In scenario of type A (cf. Fig. 1.4), the membrane marker is allowed to redistribute to steady state when further membrane traffic does not cause any further redistribution of label

between the plasma membrane and endosomes. The distribution of membrane marker is constant. This is followed by endocytic uptake of HRP for increasing lengths of time. For each time point colocalisation of the two markers is determined by measuring the degree of detergent solubility of the membrane marker after the DAB-crosslinking reaction as mediated by the

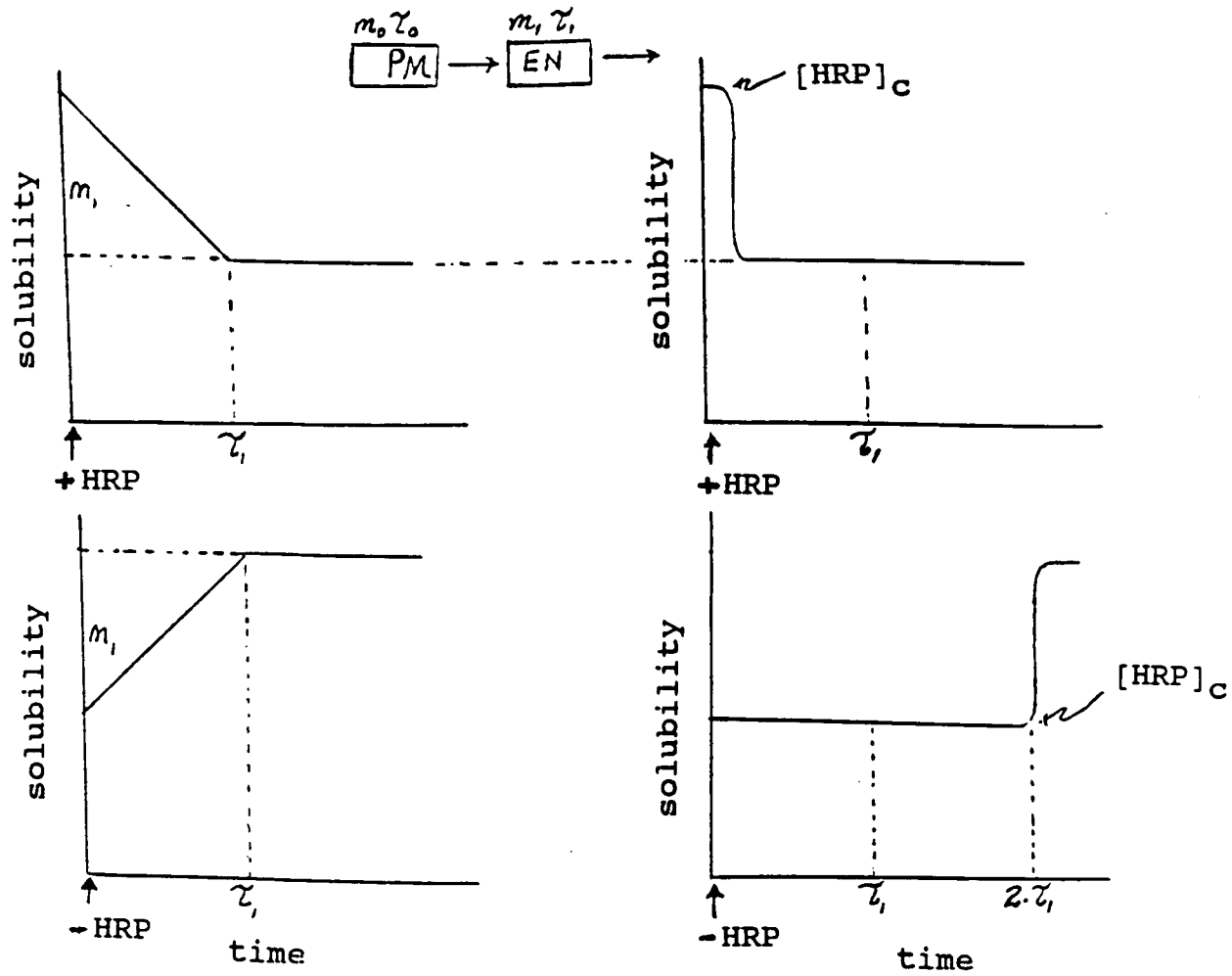

Fig. 1.4. Scenario of type A to distinguish between sequential or random processing of endosomes: ^3H distribution at steady state; chase HRP in or out of endosome. PM: plasma membrane; EN; endosome; m: pool size with respect to marker; τ_1: residence or turnover time. [HRP]c: critical concentration of HRP below which no crosslinking occurs.

A sequential behaviour of the endosome compartment will result in a gradual decline in detergent solubility of the label until the entire compartment can be crosslinked after a certain time of HRP uptake. Such a gradual decline does not have to be linear but will depend on the actual steady-state distribution of the membrane marker within the sequential stages of the endosome compartment. If the internalized HRP is chased out of the endosome compartment towards the lysosomes, the detergent solubility in the case of sequential processing will increase gradually until, ideally, it reaches maximum after the same period it took to reach maximal crosslinking.

In the case of random behaviour, no significant drop in detergent solubility of the label will be observed until after a lag when the concentration of the HRP in the "random" bag has reached the minimal concentration, $[HRP]_c$ (critical concentration), which is required to cause crosslinking. The detergent solubility of the label will drop abruptly, as the entire compartment is crosslinked. In the case of a chase of HRP towards lysosomes, there will be a much longer lag until the concentration of the HRP in the randomised pool has declined down to the critical concentration ($[HRP]_c$), when solubility will rise abruptly back to its maximum level. The actual time value of the lag will depend both on the turnover time, τ_1, of the HRP in the randomised endosome, as well as on the concentration at which HRP has been taken up as a fluid-phase marker. For example, after each turnover time, τ_1 , the concentration of HRP in the random endosome pool will decrease

by a factor of about 70% to 1/e = 1/2,7 of its value at the beginning of the considered interval; i.e. after an interval of 2 x τ_1 the concentration of HRP will have dropped to $1/e^2$ or about 10%. In the example indicated in Fig. 1.4, $[HRP]_c$ is reached after a drop by $1/e^2$, i.e. after 2 x τ_1.

In a different scenario of type B (Fig. 1.5), the endosome compartment can be filled first with HRP, followed by labelling the plasma-membrane glycoconjugates with radioactive marker. The membrane marker is then internalised into the endosome, while HRP is chased out of the endosome compartment.

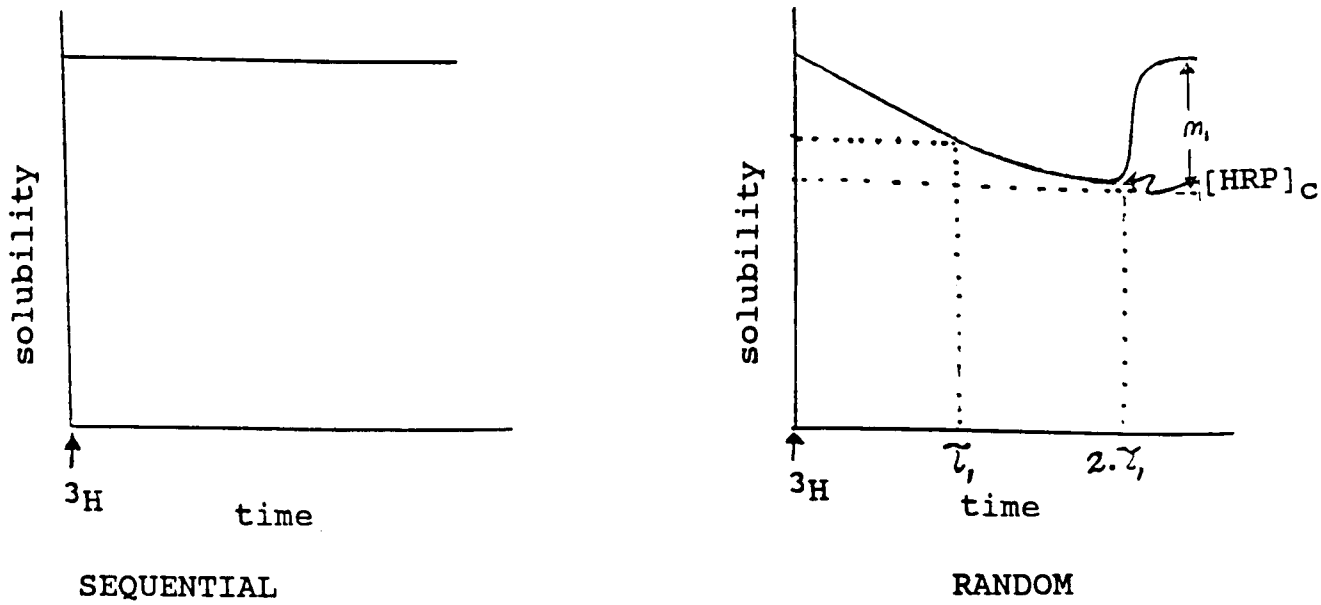

Fig. 1.5. Scenario of type B to distinguish between sequential or random processing of endosomes: Fill endosome with HRP, chase membrane marker into and HRP out of the endosomes (cf. legend of Fig. 1.4 for further details).

In the case where the endosome is processed in a sequential manner, the two markers will (ideally) not meet in a common compartment, and therefore the detergent solubility of the

membrane marker will stay constant at maximum.

A random behaviour of the endosome compartment will lead to a gradual decline in the detergent solubility as the membrane marker accumulates intracellularly with first-order kinetics. When the level of HRP in the crosslinking compartment has decreased to the critical concentration $[HRP]_c$ (which is the minimum concentration necessary to cause crosslinking in the 'random bag'), the detergent solubility of the membrane marker will abruptly return to its maximum level.

Finally, in scenario of type C, the endosome compartment can be first filled with HRP, followed by labelling of the plasma-membrane glycoconjugates with radioactive marker, which is subsequently internalised in the presence of extracellular HRP (Fig. 1.6). The constant HRP distribution is equivalent to steady state.

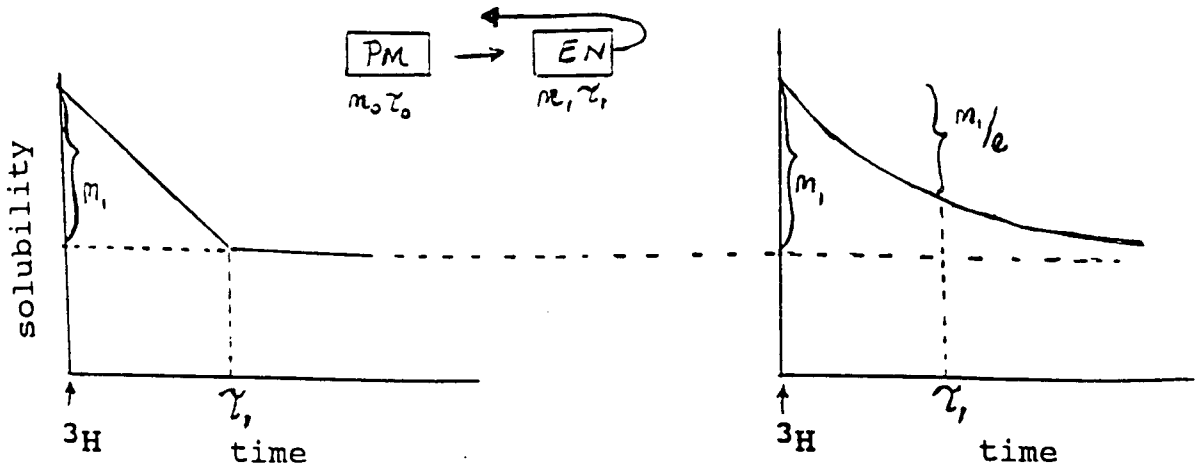

SEQUENTIAL RANDOM

Fig. 1.6. Scenario of type C to distinguish between sequential or random processing of endosomes: HRP at steady state; chase plasma-membrane marker into endosome (cf. legend to Fig. 1.4 for details).

In the case of sequential endosome behaviour, the detergent solubility of the membrane marker will decrease in a linear way, reaching maximum crosslinking after the time needed to traverse the endosome compartment (τ_1).

In the case of random behaviour of the endosome, the detergent solubility of the membrane marker will also decrease, but in an exponential way. This is due to simultaneous recycling from the 'random' bag.

CHAPTER 2

METHODS

2.1 CELLS

2.1.1 Cell culture

Cells of mouse macrophage cell line, $P388D_1$ (cf. 24), were grown at 37°C into suspension from a confluent monolayer culture in RPMI medium buffered with HCO_3, containing 10% heat inactivated fetal calf serum (Highveld or State Vaccine Institute, Pinelands, 56°C, 30 minute), 5% CO_2, 100 IU/ml penicillin and 0,1 mg/ml streptomycin.

After a growth period of not longer than 24 h in fresh medium, cells were collected from suspension by centrifugation in a table-top centrifuge (BECKMAN MODEL TJ-6) for 5 minutes at 1000 rpm in the cold. The cells were first washed twice in 30 ml Hepes-buffered RPMI medium containing BSA at 1 mg/ml (RPMI-BSA). For experimentation, about 70-150 x 10^6 cells were normally used.

2.1.2 Cell viability meaurements

The cell viability was routinely measured after harvesting cells and throughout experimental procedures. This was done by the trypan-blue exclusion assay (41). Trypan blue (0,5%) was added (1:2) to cell samples to be observed in a bright field microscope. Membrane damaged cells stained light purple-violet, whereas undamaged cells appeared translucent. If viability was less than 90%, cells were discarded.

2.1.3 Cell-surface labelling

Labelling was done on ice, essentially as before (38), with minor modifications. Washed cells were resuspended at 1,0 - 1,5 x 10^8 cells/ml in HeS-BSA buffer (10 mM Hepes pH 7.4, 140 mM NaCl, 1 mg BSA/ml) containing ß-galactosidase (0.1 U/ml, a crude enzyme mixture, prepared from Streptococcus pneumoniae, also containing neuraminidase activity) for 10 minutes on ice. The cells were then washed in 3 x 10 ml HeS and resuspended again to 1 ml in HeS-BSA containing either 10-20 µl UDP (6-^{3}H) galactose (ammonium salt; 15-20 Ci/mmol; 1 mCi/ml; Amersham) or 100 µl UDP-(U-^{14}C) galactose (lithium salt, >200 mCi/mmol; 25 µCi/ml; Amersham) and $MnCl_2$ (5 mM). The reaction was started by adding galactosyltransferase (0,5 U/ml, Sigma). After 30 minutes on ice, the reaction was stopped by 10-fold dilution in HeS or Hepes buffered RPMI medium with BSA (1 mg/ml), followed by washing again in 3 x 10 ml RPMI-He-BSA.

2.1.4 Removal of label from cell surface

Enzymatic hydrolysis of cell-surface label was done essentially as before (38). After washing the cells in RPMI-He-BSA, samples (~4-7x10^6 cells) were resuspended to 0,5 ml in the same buffer medium containing ß-galactosidase (0,2 U/ml) for 30 minutes on ice. After dilution to 5 ml, the fraction of label released was determined by comparing the radioactivity in an aliquot of total cell suspenion to that in a corresponding aliquot of supernatant after pelleting the cells by centrifugation for 5 minutes at

1000 rpm. The cells were then washed in 2x10 ml Hepes saline.

2.2 HRP ASSAY

A 50 μl aliquot of each sample was added to 0,5 ml of substrate solution (2,2-azino-di-3-ethylbenzthiazoline sulphonate (ABTS), Amersham International, at 0,55 mg/ml, 0,003% H_2O_2, 20 mM phosphate citrate [pH 4.3], 150 mM NaCl, and 0,1% Triton X-100). After 30 minutes at room temperature, the reaction was stopped by addition of 0,5 ml of citric acid (100 mM) containing NaN_3 (0,01%). Reaction product was measured via absorbance at 420 nm.

2.3 DETECTION OF RADIOACTIVITY

All samples (100-200 μl) were either counted directly in 5 ml plastic vials or put onto oxidiser pads. Samples on pads were converted to tritiated water (^3H_2O) and $^{14}CO_2$ by combustion in a sample oxidiser (Tri-Carb, Packard). Samples were measured by scintillation counting to an accuracy of about 2σ = 1%.

2.4 CELLS HOMOGENISATION

(i) Cells were resuspended in 3 ml homogenisation buffer, STE (0,25 M sucrose/10 mM Tris HCl, pH 7.4 / 1 mM EDTA]) and passed through a cell cracker (cf. 24) (10 strokes) in the cold. As seen under the light microscope, about ~98% of the cells were broken as observed via trypan blue staining. The homogenate was centrifuged at 2000 rpm x 10 minutes to sediment the nuclei and

unbroken cells. Post-nuclear supernatant (PNS) was applied on a sucrose step-gradient and centrifuged in a SW40 rotor (28000 rpm x 60 minutes) to isolate an endosome-enriched fraction.

(ii) In other experiments mellitin (40) was used for breaking cells instead of the cell cracker. Cells were resuspended in 5 ml mellitin solution (1 μg/ml in STE buffer) in the cold, to allow embedding of mellitin into the plasma membrane. The suspension was then centrifuged (5 x 1000 rpm) and supernatant was removed. Cells were resuspended again in STE buffer (1 ml) and pipetted up and down five times. The homogenate was made up to 8 ml with STE buffer (cold) and centrifuged at 2000 rpm for 10 minutes. The PNS was loaded and centrifuged on a sucrose step-gradient as before, to isolate endosome-enriched fractions. A similar degree of breaking was achieved with this method (~ 96%).

2.5 DAB CROSSLINKING AND DETERGENT SOLUBILIZATION

Diaminobenzidine (DAB) solutions were prepared at a concentration of 3 mg/ml (1 Tablet of 10 mg was dissolved in 3,3 ml of STE buffer, resulting in pH ~5 which was carefully adjusted to pH 7.2-7.4 with about 35 μl of 2 M NaOH). This solution, which is light brown in colour, and contained insoluble remnants, was filtered through a 0,22 μm millipore filter and protected from light, and kept in the fridge before use (usually less than 2 hours). Depending on the procedures before, DAB crosslinking was done differently.

(i) Samples of 1,5 ml of endosome-enriched fractions were diluted to 3 ml in fractionation buffer, STE. These samples were divided into two 1,5 ml fractions, one of which served as negative control without crosslinking (background insolubility). DAB solution (0,3 ml) was added to the 1,5 ml sample (final DAB concentration 0,5 mg/ml) and the reaction occurred at room temperature for 30 minutes in the dark, in the presence of 18 μl H_2O_2 (0,3%), or absence of H_2O_2 for negative controls. The reaction was stopped by addition of 90 μl BSA (20 mg/ml). 20 μl Triton X-100 (1%) or SDS (final concentration 1%) was added immediately afterwards.

(ii) Intact cells (~ 4-6 x 10^6 cells) were washed in 2x10 ml HeS and resuspended in 1 ml HeS on ice, and DAB solution (180 μl) added. Cells were incubated for 30 minutes on ice in the dark, to allow permeation of DAB into the cells. After rapid warming to room temperature, where the DAB reaction occurs more efficiently, 12 μl H_2O_2 (0,3%) was added for a further 15 minutes in the dark. The reaction was stopped by addition of 5 ml HeS containing BSA (1 mg/ml) and cells collected by centrifugation at 1000 rpm for 5 minutes. The cells were resuspended in HeS (3 ml) buffer, containing 1% Triton X-100 and 0,3 mg/ml DNAse. The cells were homogenised, and the mixture incubated for 15 minutes at 37°C to facilitate the DNAse action. Cells, washed after the DAB reaction and resuspended to 1 ml in HeS, could be stored overnight (in the presence of 0,03 M NaN_3) in the fridge before detergent treatment the next day.

Crosslinking was determined by separating the detergent soluble from insoluble material by centrifugation at 28000 rpm x 60 minutes in a SW40Ti rotor (Beckman) on a 35% sucrose cushion: 1.5 ml samples were overlayered on 10 ml of 35% sucrose; 100 μl aliquots (double samples) were taken from the overlayered volume before centrifugation to represent the total radioactive material in the sample; similar aliquots were taken after centrifugation to represent the detergent-soluble radioactive material; aliquots were put on pads for combustion prior to scintillation counting.

2.6 CALCULATION OF THE "FRACTIONAL SOLUBILITY"

In order to determine the efficiency of intracellular crosslinking by DAB, of membrane marker in compartments containing HRP, only intracellular marker had to be considered. This became relevant because only about 85-90% of the non-internalized membrane marker could be removed by glycosidase treatment. The remaining 10-15% on the cell surface, which was not susceptible to subsequent crosslinking, caused a background signal for solubility of label, and had to be accounted for by calculating the "fractional solubility".

The fraction of cell-surface label (no internalization, cells kept on ice) which could be removed by glycosidase treatment was measured as β_o.

The fraction of cell-surface label which could be removed from cells after membrane internalization for a time, t, was measured as $ß_t$.

Therefore, the fraction of internalized label at time, t, was calculated as (1-ßt/ßo), with the complementary fraction of label remaining on the cell surface, viz. ßt/ßo.

Treatment with glycosidase, removing the fraction ßo of cell-surface label, left (1-ßo).ßt/ßo of the total label on the cell surface.

The intracellular label, as a fraction of the total label remaining cell associated, was

$$(1-ß_t/ß_o) \;/\; [(1-ß_t/ß_o) + (1-ß_o).ß_t/ß_o].$$

This was the fraction that could be expected to become detergent insoluble due to intracellular crosslinking by DAB if all intracellular label resided in HRP containing organelles, and in view of residual label on the cell surface. It was to be the maximally expected degree of crosslinking, X_{max}.

The measured degree of crosslinking, X_{meas}, had to be compared to X_{max}, i.e. X_{meas}/X_{max}. (X_{meas} was obtained by normalising the measured degree of crosslinking for less than 100% solubility obtained for the negative control samples).

The "fractional solubility" was expressed as $(1-X_{meas}/X_{max})$.

2.7 CHEMICALS, ENZYMES AND CULTURE WARE

All culture plastic ware was from Greiner-Labortechnik, Germany or from Falcon, Becton Labware, New Jersey. Penicillin G, Streptomycin sulphate and Foetal Calf Serum were from Highveld and State Vaccine Institute, Cape Town, South Africa. Bovine Serium Albumin (Boehringer - W. Germany). Horse Radish Peroxidase (Seravac & Sigma Chemical Co.). Galactosyl transferase (Sigma Chemical Company). ß-galactosidase was prepared in Dept. Medical Biochemistry, University of Cape Town. UDP-D-[U-^{14}C] Galactose, Lithium salt and UDP-D-[6-^{3}H] Galactose, Ammonium salt were from Amersham, England.

CHAPTER 3

RESULTS

3.1 Efficiency of crosslinking in endosomes

The efficiency of crosslinking of internalised membrane marker was determined by comparing the maximal degree of detergent insolubility after DAB crosslinking, with the maximal detergent solubility of membrane marker as obtained in the absence of any crosslinking (negative controls) (Fig. 3.1). These experiments were first done for isolated endosomes in order to allow comparison with previous results from other authors (35).

To establish the scenario for the highest degree of crosslinking to be expected, plasma-membrane marker (^{3}H-labelled) was internalised into the endocytic pathway to steady state, while at the same time HRP was endocytosed to fill all membrane compartments en route to 2° lysosome. At steady state only about 17% of total membrane marker was on intracellular membranes, with the bulk of the label (83%) remaining on the plasma membrane: As this label was not to be crosslinked in the absence of extracellular HRP, it would result in a high background of detergent soluble label. Therefore, it was first removed from the cell surface by treatment with glycosidases prior to the DAB reaction. In order to obtain a crude organelle fraction containing HRP-loaded endosomes, in the absence of free HRP due to organelle breakage during cell fractionation, membranes of a post-nuclear supernatant (PNS) were passed

A

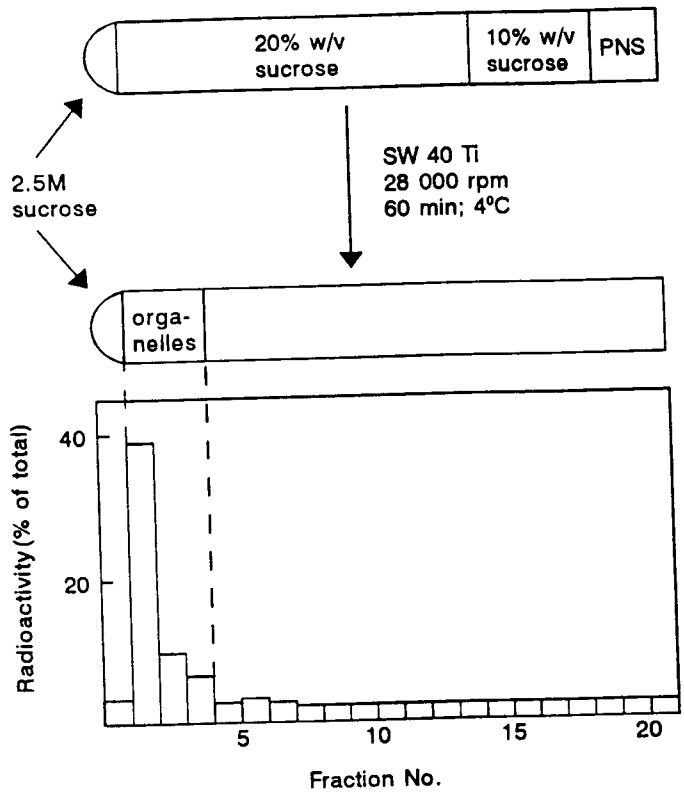
20% w/v sucrose
10% w/v sucrose
PNS
2.5M sucrose
SW 40 Ti
28 000 rpm
60 min; 4°C
orga-nelles
Radioactivity (% of total)
40
20
5
10
15
20
Fraction No.

B

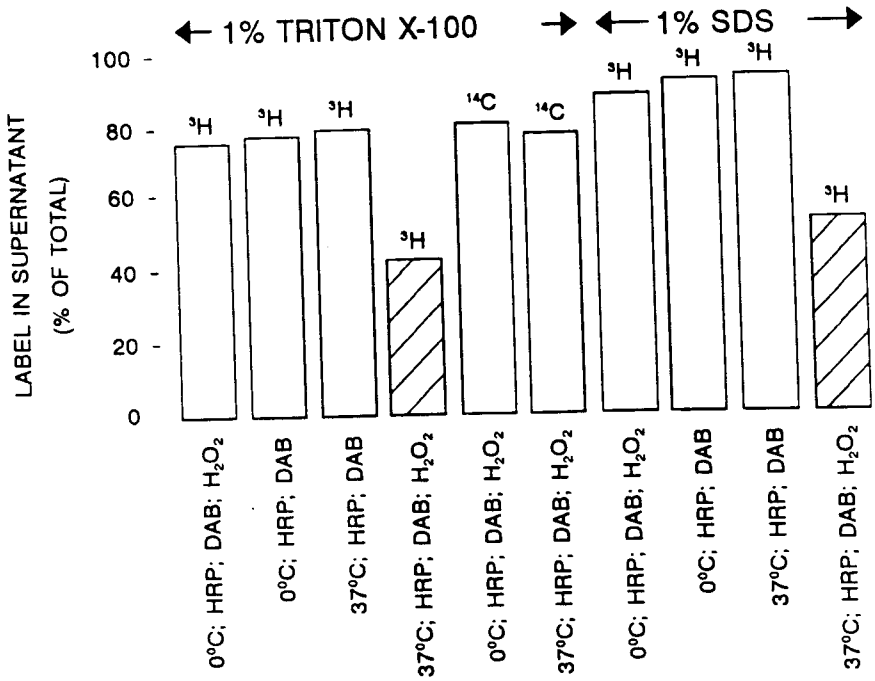
← 1% TRITON X-100 →
← 1% SDS →
LABEL IN SUPERNATANT (% OF TOTAL)
100
80
60
40
20
0
³H
³H
³H
³H
¹⁴C
¹⁴C
³H
³H
³H
³H
0°C; HRP; DAB; H2O2
0°C; HRP; DAB
37°C; HRP; DAB
37°C; HRP; DAB; H2O2
0°C; HRP; DAB; H2O2
37°C; HRP; DAB; H2O2
0°C; HRP; DAB; H2O2
0°C; HRP; DAB
37°C; HRP; DAB
37°C; HRP; DAB; H2O2

FIG. 3.1

FIG. 3.1 Evidence that peroxidase catalysed oxidation of DAB within endosomes renders their membrane glycoconjugates detergent insoluble. After labelling the plasma membrane with [^{3}H]Gal, cells were resuspended in medium containing HRP (1-2 mg/ml). Equal portions of the cell suspension were incubated for 30 minutes at 37°C or kept on ice, respectively. Cells were washed in the cold and treated with ß-galactosidase which removed about 90% of the cell surface label. In some experiments cells were then labelled with [^{14}C]Gal to provide a marker for non-internalised membrane. After homogenising in a cell cracker (cf. Methods), the post-nuclear supernatant (PNS) was applied on a sucrose gradient (3.1A) and endosome-rich fractions 1-7 (containing about 66% HRP activity) were recovered. Endosomes were either incubated with DAB/H_2O_2 or DAB without H_2O_2 as the control, and solubilised by addition of Triton X-100 (1%) or SDS (1%), and lysates were centrifuged over a cushion of 35% sucrose. Detergent solubility was measured as the fraction of the label remaining in supernatant after centrifugation (3.1B). Radioactivity was measured after conversion to $^{3}H_2O$ and $^{14}CO_2$ and are presented as a mean of several determinations.

through a sucrose solution. This washing step did not involve elimination of other membranes from endosomes.

For isolated endosomes, the solubility of the membrane marker after crosslinking with DAB was 45% or 55%, depending on whether Triton X-100 or SDS, respectively, was used for solubilisation (cf. Fig. 3.1B).

To obtain a measure for the maximal solubility, and in view of the above results being different for the two detergents used to dissolve the membrane fractions, a number of negative controls were analysed. The DAB reaction could be rendered ineffective by a number of omissions: absence of H_2O_2, absence of HRP, absence of label on HRP containing membranes (0°C, i.e. no internalization of cell-surface label), or a combination of these.

The most relevant and direct negative control was obtained by applying a second cell-surface marker, [^{14}C]Gal, after cells had internalised the first, [^{3}H]Gal, into their HRP-containing endosomes. This, therefore, provided an internal negative control. As shown in Fig. 3.1B, all negative controls showed similar high solubilities of about 80% or 90%, again depending on whether Triton X-100 or SDS was employed for solubilisation, respectively.

The maximal solubility in Triton X-100 of about 75% has been

reported for radioactive transferrin in HRP containing endosomes (35).

For isolated endosome in a crude membrane fraction, the present results thus suggested a maximal degree of crosslinking of between 45% and 40% when normalised for 100% solubility of the negative controls. Part of this low degree of crosslinking might be due to the presence of labelled membrane of broken endosomes which had lost their HRP contents (cf. HRP recovery of ≈66%, legend to Fig. 3.1.). A further contribution to non-crosslinked label would be expected from label remaining on the cell surface after treatment with ß-galactosidase (about 14% in comparison to about 13% on intracellular membranes; cf. Fig. 3.2A).

Since the present work attempted to make a quantitative analysis of membrane dynamics, the problem of endosome breakage during cell fractionation was avoided by adapting the crosslinking assay to intact cells. As shown in the next section, quantitatively similar results could be obtained.

3.2 Efficiency of crosslinking when intact cells are used

To determine the crosslinking efficiency when performing the DAB reaction for intact cells, the same endocytosis protocol was followed as in the previous section. Membrane marker was internalised for increasing times into the endocytic pathway in the presence of HRP (or without HRP for negative control) (Fig. 3.2).

The degree of internalisation of cell-surface label was determined by treating cells with glycosidases in order to remove selectively cell-surface label. As shown in Fig. 3.2A, glycosidase treatment removed about 86% of the label when this was all on the cell surface (at t=0, prior to internalisation). This value was used to represent 100% of the label on the cell surface and all values for the later time points were normalised accordingly. As shown in Fig. 3.2B, about 16% of the label was redistributed to intracellular membranes after 16 minutes.

As shown in Fig. 3.2D the maximal crosslinking obtained when intact cells were used was about 28%. In other experiments a similar or lower value was obtained, cf. Fig. 3.2E. This value was lower as compared to the ones obtained for isolated endosomes in Section 3.1 (40% - 45%), which was obtained at steady state plasma membrane redistribution (i.e. about 17% plasma membrane on intracellular membranes). In view of this, potential crosslinking at different times was calculated as it would have been expected for internalised label only, without any contribution by (soluble) label remaining on the cell surface after hydrolase treatment. This potential crosslinking, when compared to the observed values as in Fig. 3.2D, was used to calculate the fractional solubility (cf. Methods).

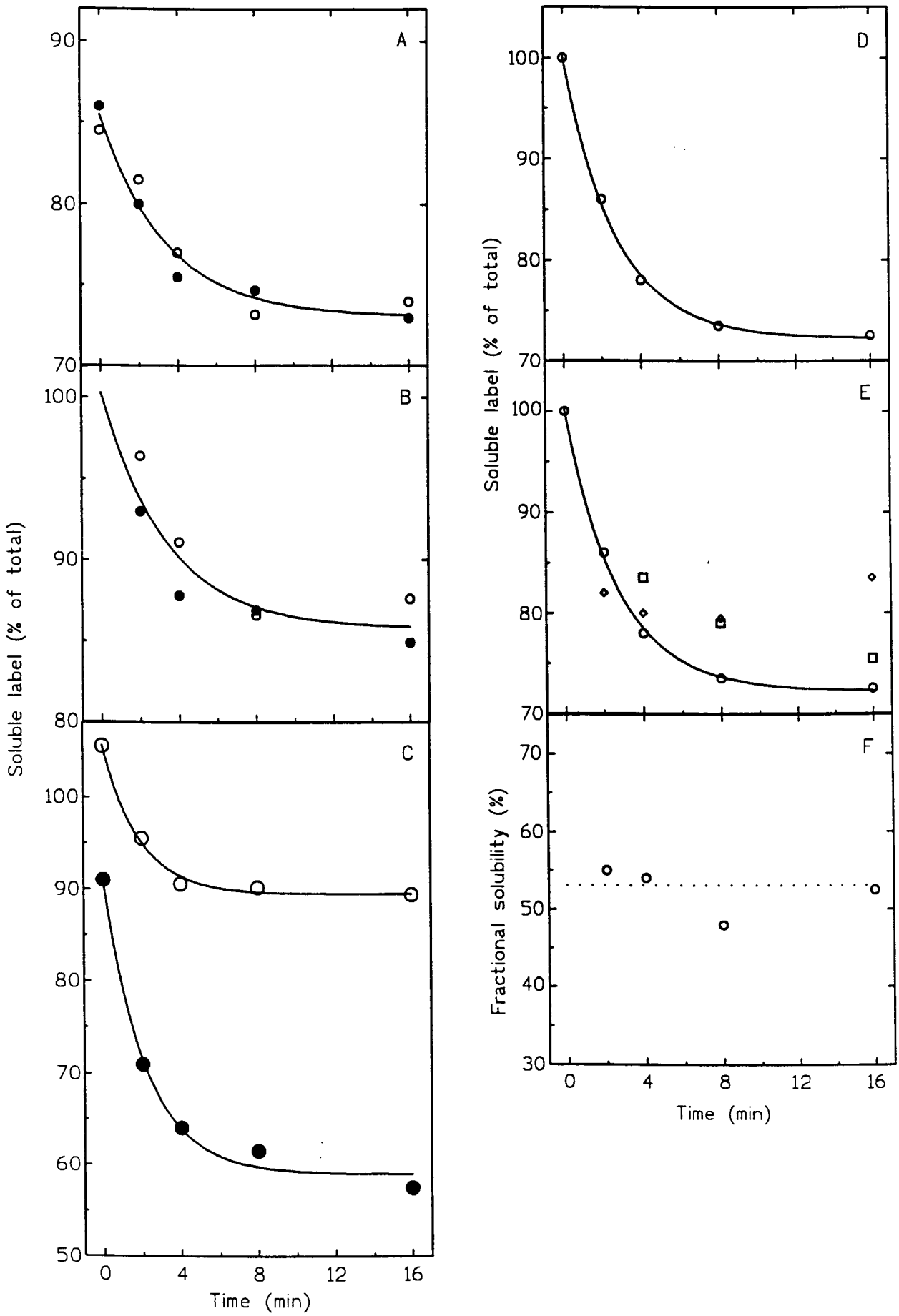
A
B
C
D
E
F
Soluble label (% of total)
Fractional solubility (%)
Time (min)
90
80
70
100
60
50
40
30
0
4
8
12
16

FIG. 3.2

FIG. 3.2: Intra-cellular crosslinking of plasma membrane glyco-conjugates, internalised in the presence of HRP. A cell suspension was divided into two equal portions and incubated for 30 minutes at 37°C in the presence (closed symbols) or absence (open symbols, except in D and E) of HRP (1 mg/ml). After cooling on ice, cells were pretreated with ß-galactosidase (0.1 U/ml) for 10 minutes, washed, and the cell surface was labelled with [^{3}H]Gal (closed symbols) or [^{14}C]Gal (open symbols, except in D, E and F, respectively. Cells were resuspended in the presence (^{3}H, closed symbols) or absence (^{14}C, open symbols) of HRP, and at t=0 (before warming), and at the indicated times at 37°C, samples were taken by cooling on ice. Cells were washed free from external HRP, prior to combining ^{3}H- and ^{14}C-labelled samples from the corresponding time points. Each of these samples was treated with ß-galactosidase (0.2 U/ml for 30 minutes on ice) to release the cell-surface label as shown in A, as a measure for the degree of internalisation. The fraction of label that could be released from the cells without internalisation after labelling (values at t=0 in A) was normalised to represent 100% of label on the cell surface (value at t=0 in B) and all other values at t>0 within each series were normalised accordingly, to indicate the fraction of label remaining on the cell surface (with the complimentary fraction internalised), as shown. The samples (^{3}H and ^{14}C combined) for each time point were then treated with DAB/H_2O_2, followed by resuspension in detergent (Triton X-100 for circles and squares, SDS for diamonds) and homogenisation in the cell cracker (cf. Methods). Detergent solubility was measured as the fraction of

the total label remaining in the supernatant after centrifugation on a 35% sucrose cushion for 60 minutes at 10^5 x g (cf. Methods). Radioactivity was measured after complete separation of isotopes as ^3H_2O and $^{14}CO_2$. Solubility values for ^3H label (with HRP above, closed symbols in C) were corrected for intra-experimental variation by dividing with the corresponding solubility values as measured for ^{14}C-label as internal negative control (without HRP above, open symbols in C). The $^3H/^{14}C$ solubility ratio for the t=0 pair was taken to indicate 100% solubility (t=0 in D) and all other ratios (for t>0, within the same experiment) were normalised accordingly, as shown in D. Variation between independent experiments is shown in E when using Triton X-100 (squares, and circles as from D) or SDS (diamonds) as the solubilising detergent. When the solubility is calculated with respect to only internalized label, i.e. disregarding the contribution of label remaining on the cell surface as resistant to removal with hydrolases (complementary to the intercept on the ordinate in A), the obtained 'fractional solubility' as shown in F (cf. Methods).

As shown in Fig. 3.2F, the fractional solubility was about 50%, and therefore quantitatively similar to what was obtained for isolated endosomes (cf. Fig. 3.1B).

The experimental protocol, as described above, represented the scenario of type C (Fig. 1.6). The observation that label redistributed to intracellular compartments with first-order kinetics (Fig. 3.2B), as was also reflected by the first-order decrease in solubility (Fig. 3.2D) was indicative of a random processing of membrane marker in endosomes.

3.3 Endocytic uptake of HRP, followed by internalisation of plasma-membrane glycoconjugates, leads to early intermingling of the two markers in the endosome

Experiments were performed according to scenario type B (Fig. 1.5): The membrane was internalised at 37°C for increasing times into the endocytic pathway filled with HRP (or without HRP pre-loading for negative control). Unlike in the previous section, membrane marker was internalised in the absence of external HRP, i.e. while HRP was chased along the endocytic pathway. For this determination, and others following thereafter, the DAB reaction was performed on intact cells.

First, the degree of internalisation of cell-surface label was determined by treating with glycosidases in order to remove selectively cell-surface label. As shown in Fig. 3.3A, glycosidase treatment removed about 90% of the label when this

was all on the cell surface (i.e. at t=0, prior to internalisation). If this value is taken to represent 100% of the label on the cell surface as before, and all values for later time points normalized accordingly, then about 14% of the label would be redistributed to intracellular membranes after 40 minutes.

The data in Fig. 3.3C suggest that some intermingling observed (via crosslinking) of newly internalized membrane marker with previously endocytosed HRP occurred. This can be seen by comparing the curve in Fig. 3.3C with the contemplated outcomes as envisaged for scenario of type B (Fig. 1.5). The time dependence displayed by the data in Fig. 3.3C is reminiscent of the curve as suggested in Fig.1.5.

A more quantitative assessment of the degree of intermingling was obtained by calculating the fractional solubility. As shown* in Fig. 3.3D, minimum solubility was achieved as soon as membrane marker was internalized after HRP uptake. As HRP was chased along the endocytic pathway towards secondary lysosomes, the solubility of membrane marker gradually increased. This finding provides direct evidence for the random processing of membrane marker in endosomes, in agreement with the first-order kinetics observed in the previous section.

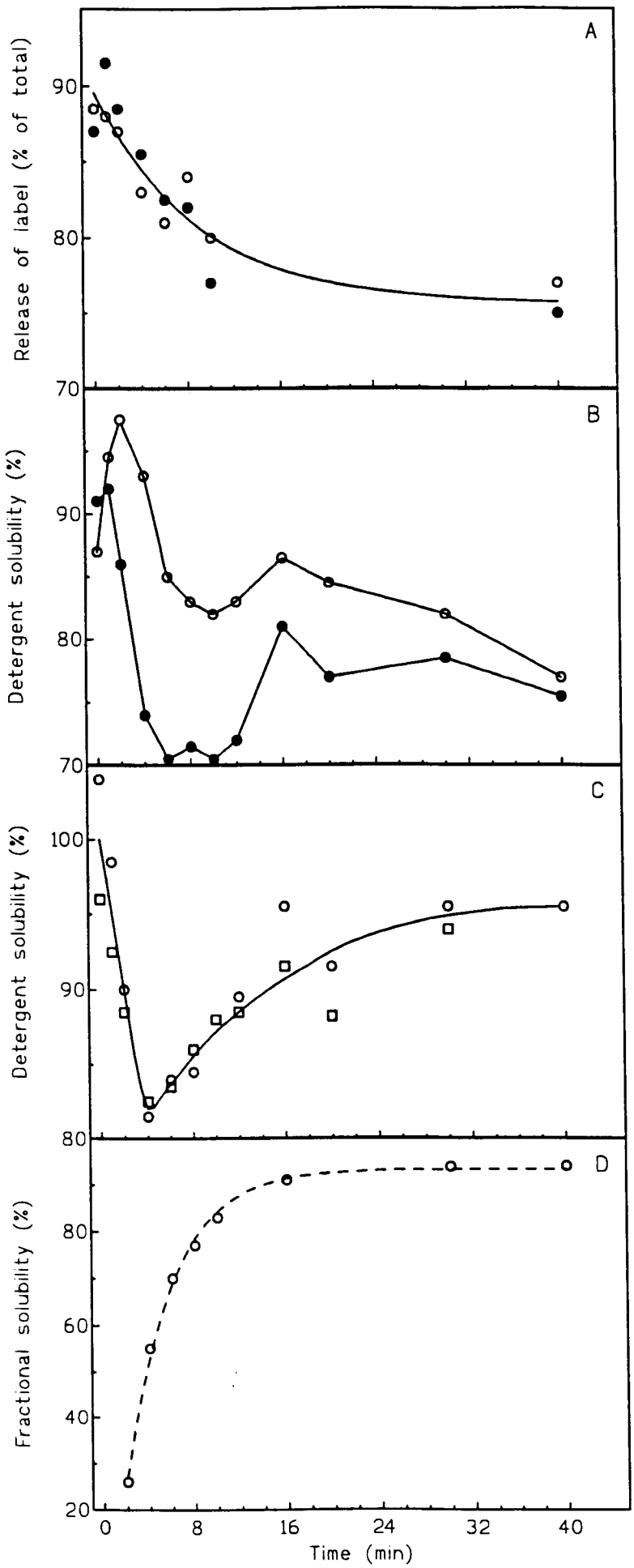
A
B
C
D
Release of label (% of total)
Detergent solubility (%)
Detergent solubility (%)
Fractional solubility (%)
90
80
70
90
80
70
100
90
80
80
60
40
20
0
8
16
24
32
40
Time (min)

FIG. 3.3

Fig. 3.3: Endocytic uptake of HRP, followed immediately by internalisation of labelled plasma-membrane glycoconjugates. A cell suspension was divided into two equal portions and incubated in the presence (closed symbols) or absence (open symbols, except in C and D) of HRP (1 mg/ml) for 30 minutes at 37°C. After cooling on ice, cells were pretreated with ß-galactosidase (0.1 U/ml) for 10 minutes, washed and the cell surface labelled with [^{3}H]Gal (closed symbols) or [^{14}C]Gal (open symbols, except in C), respectively. Cell suspensions were both resuspended in the absence of HRP, and at t=0 (before warming) and at the indicated times at 37°C, samples were taken by cooling on ice, followed by combining ^{3}H- and ^{14}C-labelled samples from the corresponding time points. Combined samples were treated with ß-galactosidae (0,2 U/ml for 30 minutes on ice) to release cell-surface label as shown in A. The samples (^{3}H and ^{14}C combined) for each time point were then treated with DAB/H_2O_2, followed by resuspension in detergent (Triton X-100) and homogenisation in a cell cracker. Detergent solubility was measured as the fraction of the total label remaining in the supernatant after centrifugation on a 35% wt/wt sucrose cushion for 60 minutes at 10^5 x g (cf. Methods). Radioactivity was measured after complete separation of isotopes as $^{3}H_2O$ and $^{14}CO_2$. Solubility values for ^{3}H-label (cells previously with HRP, closed symbols in B) were corrected for intra-experimental variation by dividing with corresponding solubility values as measured for ^{14}C-label, as internal negative control (no previous loading with HRP, open symbols in B). The $^{3}H/^{14}C$ solubility ratios at different times are shown in C, squares and circles refer to independent experiments. The fractional solubility, calculated for internalized radioactivity only (cf. Methods) is shown in D.

3.4 Endocytic uptake of HRP, after internalisation of labelled plasma-membrane constituents to steady state

Experiments were performed according to the scenario of type A (Fig. 1.4). The cell-surface membrane marker was internalised into the endocytic pathway to steady state, followed by internalisation of HRP for increasing times in order to observe the kinetics by which HRP, as a contents marker, was processed along the endocytic pathway.

The fraction of membrane marker on intracellular membranes at steady state was determined by treating the cells with glycosidases. This also served to remove selectively cell-surface label in order to reduce the contribution by non-crosslinkable label. As shown in Fig. 3.4A, glycosidase treatment removed about 78% of the label and because of the steady-state situation this value did not change for samples at different time points. When corrected for surface label, remaining due to incomplete removal by glycosidase treatment (only ≈90% was removed for samples with non-internalized label), the amount of label internalised at steady state amounted to 13-14% (100-78/0.9).

As shown in Fig. 3.4C, the decrease in solubility when HRP was internalised for increasing times occurred gradually without any lag at the initial stage. According to the scenario of type A (cf. Introduction), these kinetics would suggest that HRP was processed in a sequential manner in the endosome. The change of

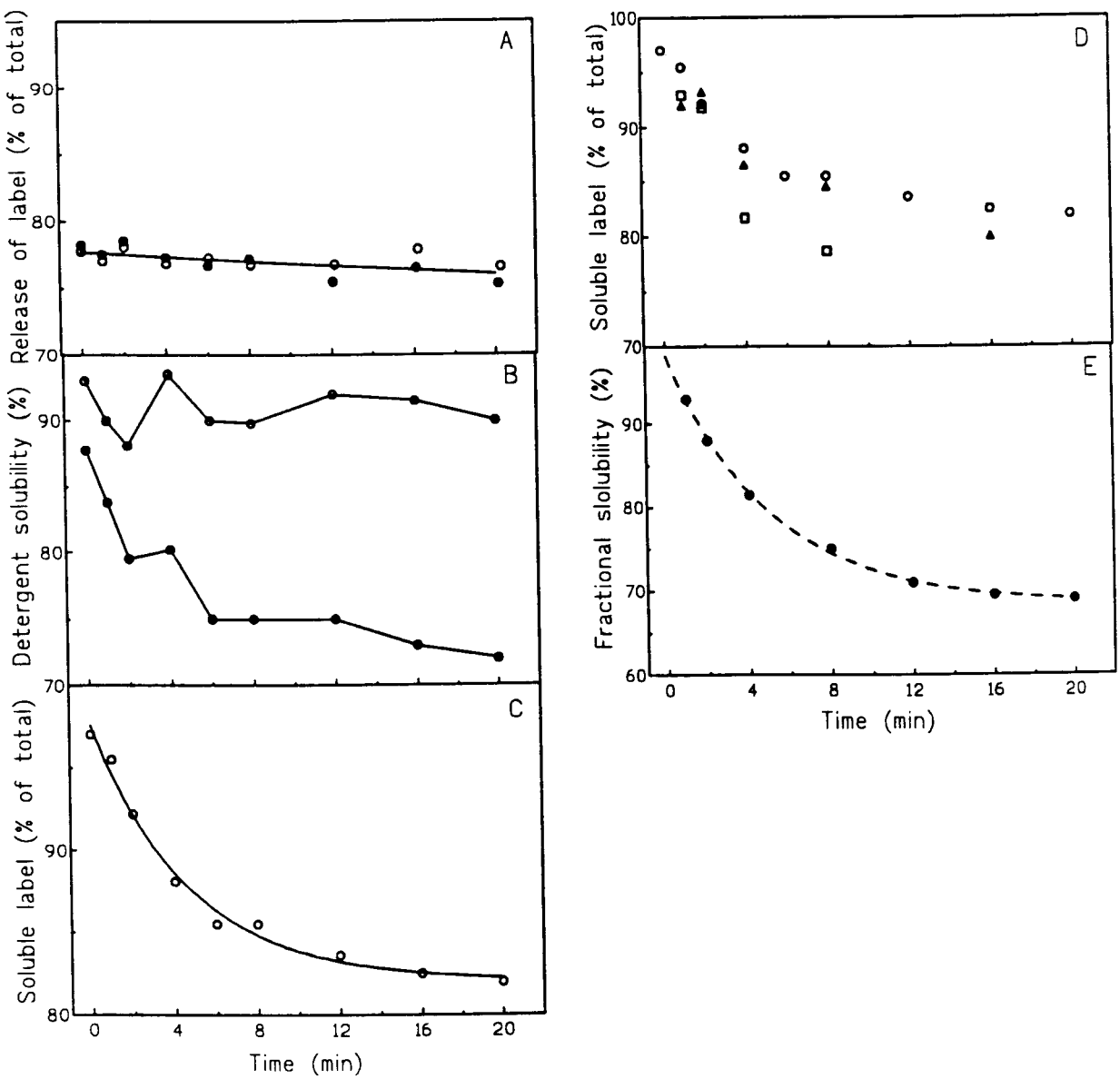
A
B
C
D
E
Release of label (% of total)
Detergent solubility (%)
Soluble label (% of total)
Soluble label (% of total)
Fractional solubility (%)
Time (min)
Time (min)

FIG. 3.4

Fig. 3.4: Redistribution of plasma membrane glycoconjugates to steady state, followed by internalisation of HRP. A cell suspension, pretreated with ß-galactosidase (0,1 U/ml) for 10 minutes, was divided into two equal portions, and the cell surface labelled with [^{3}H]Gal (closed symbols) or [^{14}C]Gal (open symbols, except in C, D and E), and incubated for about 60 minutes at 37°C to achieve a steady-state distribution of the membrane marker. HRP (1 mg/ml) was then added (closed symbols) or not (^{14}C, open symbols, except in C, D and E). At t=0 (before HRP addition) and at indicated times (after HRP addition) at 37°C, samples were taken by cooling on ice. Cells were washed free of external HRP prior to combining ^{3}H and ^{14}C labelled samples from the corresponding time points. Combined samples were treated with ß-galactosidase (0,2 U/ml for 30 minutes) on ice, to release cell-surface label as shown in A. The samples (^{3}H and ^{14}C combined) for each time point were then treated with DAB/H_2O_2, followed by resuspension in detergent (1% Triton X-100 for circles and triangles, and 1% SDS for squares) and homogenisation in the cell cracker. Detergent solubility was measured as the fraction of the total label remaining in the supernatant after centrifugation on 35% wt/wt sucrose cushion for 60 minutes (circles and squares) or filtration (triangles) (cf. Methods). Radioactivity was measured after complete separation of isotopes as $^{3}H_2O$ and $^{14}CO_2$. Solubility values for ^{3}H label (with HRP, closed symbols in B) were corrected for intra-experimental variation by dividing with the corresponding solubility values as measured for ^{14}C as internal negative control (without HRP, open symbols in B). The ^{3}H/^{14}C solubility ratio for t=0 was taken as indicating 100% solubility (t=0 in C and D) and all the other ratios (for t>0) within the same experiment, were normalised as in C and D. The fractional solubility for the data in C was calculated (cf. Methods) as shown in E.

fractional solubility (Fig. 3.4E) allowed quantitative comparison with the data in other figures.

3.5 Membrane label at steady state, and HRP chased out towards lysosomes

In order to further investigate the processing kinetics of HRP as endocytic contents marker (cf. scenario of type A, Fig. 1.4), cell-surface label was allowed to reach a steady-state distribution before HRP was added for a further 30 min at 37°C. This was followed by re-incubation at the same temperature in HRP-free medium in order to chase HRP out of the endosome compartment towards lysosomes.

As shown in Fig. 3.5A, surface label was removed by glycosidase treatment to measure the fraction of intracellular label at steady state and to reduce the interference by non-crosslinkable label. With about 74% of the label removed, in comparison with about 88% removal from cells without internalisation of label, the label distributed to intracellular membranes at steady state was calculated as about 16%, which corresponds well to other experiments.

From the data in Fig. 3.5 A,B,C, the fractional solubility was calculated (cf. Methods) as shown in Fig. 3.5D. As HRP was chased out of the endosome compartment a gradual increase in fractional solubility was observed. In comparison with the

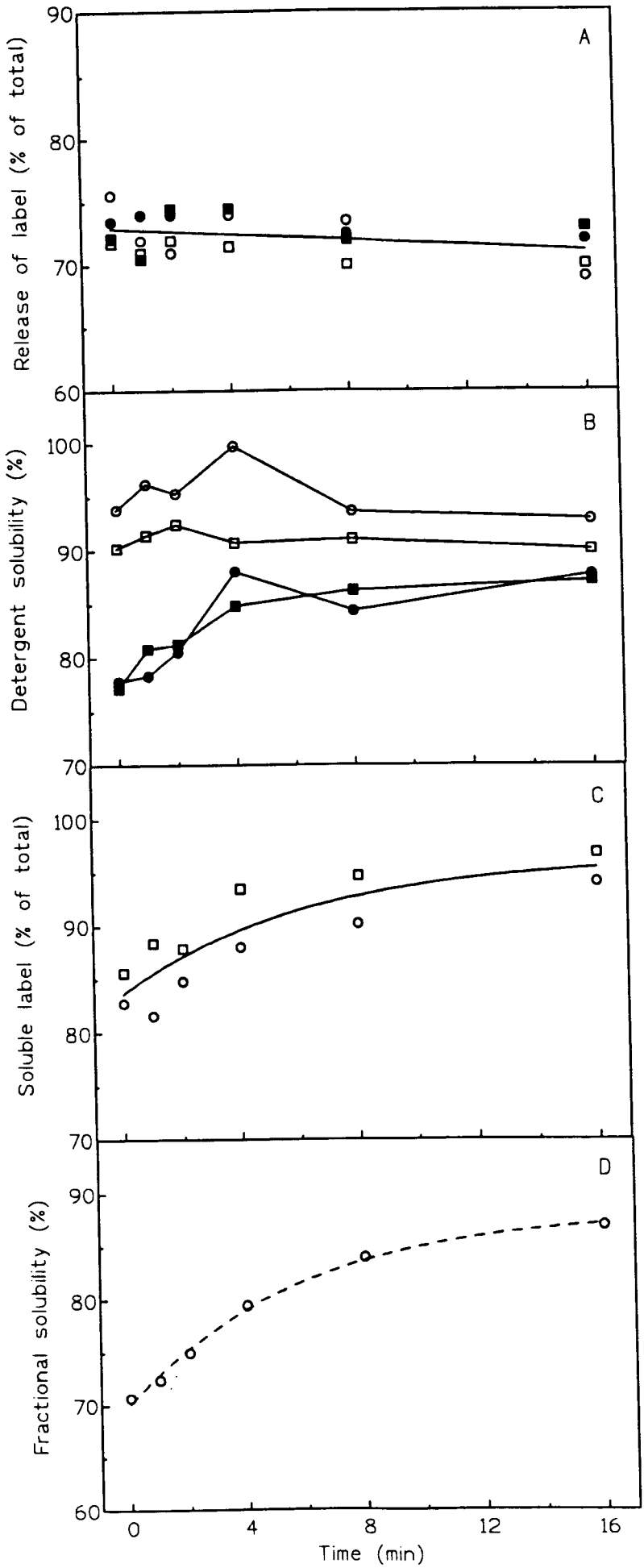
A
B
C
D
Release of label (% of total)
Detergent solubility (%)
Soluble label (% of total)
Fractional solubility (%)
Time (min)
90
80
70
60
100
0
4
8
12
16

FIG. 3.5

Fig. 3.5: Chase of HRP out of endosomes bearing a steady-state distribution of membrane marker. A cell suspension, pretreated with ß-galactosidase (0.1 U/ml) for 10 minutes and washed, was divided into two equal portions and labelled with [^{3}H]Gal (closed symbols) or [^{14}C]Gal (open symbols, except in C and D). Cells were resuspended in the absence of HRP for 60 minutes at 37°C, followed by further 60 minutes in the presence (^{3}H, closed symbols) or absence (^{14}C, open symbols) of HRP (1 mg/ml). Cells were cooled, washed of free external HRP, and the ^{3}H- and ^{14}C-labelled cells combined. At t=0 (before warming), and at indicated times at 37°C samples were taken by cooling on ice, and samples were treated with ß-galactosidase (0.2 U/ml for 30 minutes on ice) to release cell-surface label as shown in A. Squares and circles refer to independent experiments. The samples for each time point were then treated with DAB/H_2O_2, followed by resuspension in detergent (1% Triton X-100) and homogenisation in the cell cracker. Detergent solubility was measured as the fraction of the total label remaining in the supernatant after centrifugation on a 35% wt/wt sucrose cushion for 60 minutes at 10^5 x g (cf. Methods). Radioactivity was measured after complete separation of isotopes as $^{3}H_2O$ and $^{14}CO_2$. Solubility values for ^{3}H label (with HRP, closed symbols in B) were corrected for intra-experimental variation by dividing with the corresponding values measured for ^{14}C-label, as internal negative control (without HRP, open symbols in B). The ^{3}H/^{14}C solubility ratios at different times are shown in C. The fractional solubility was calculated from the data in A and C, as shown in D (cf. Methods).

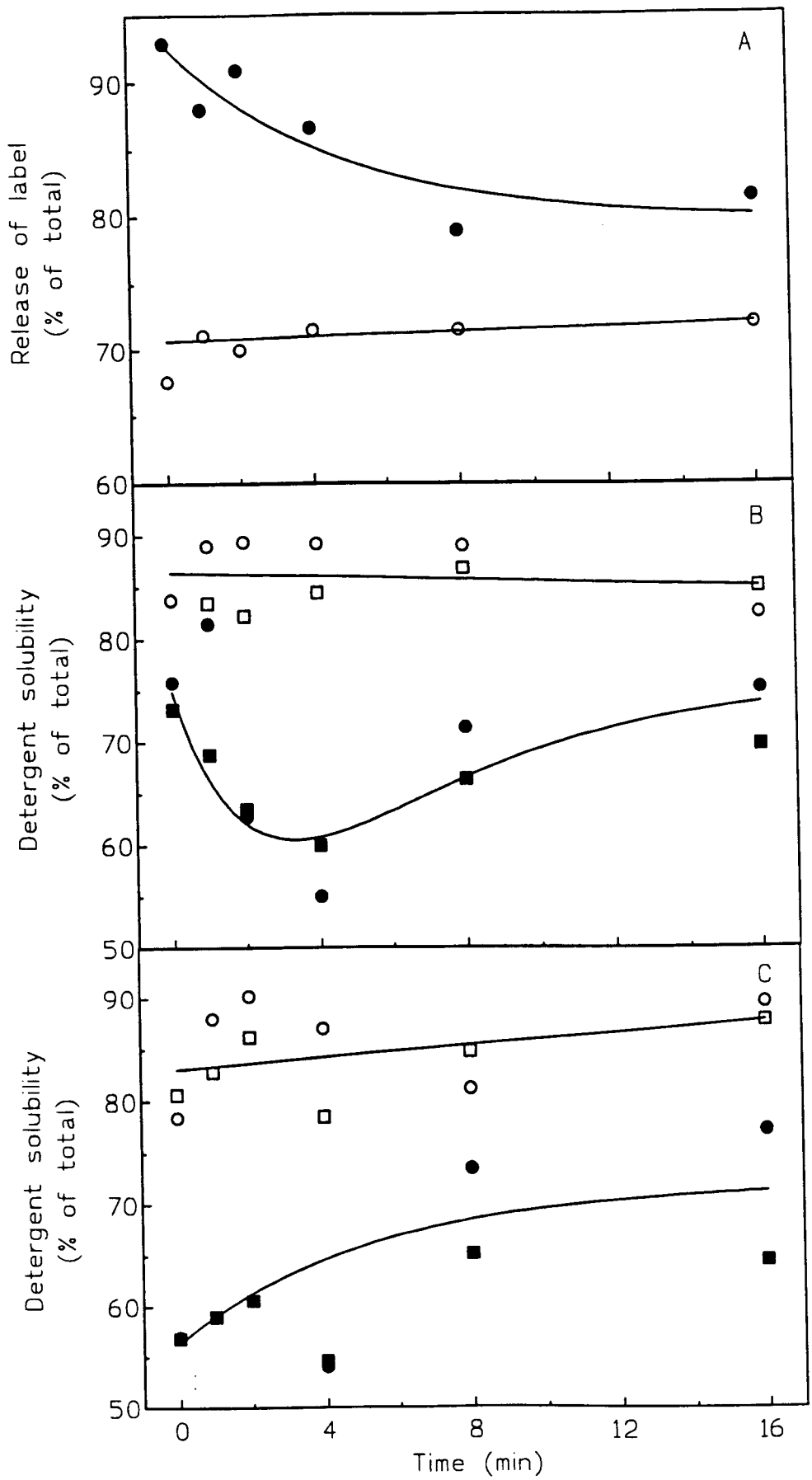
A
B
C
Release of label
(% of total)
Detergent solubility
(% of total)
Detergent solubility
(% of total)
90
80
70
60
50
0
4
8
12
16
Time (min)

FIG. 3.6

Fig. 3.6: Plasma membrane (^{3}H-labelled) internalised subsequent to a pulse of HRP in endosomes bearing membrane marker (^{14}C-labelled) at steady-state distribution. Cells were pretreated with ß-galactosidase (0.1 U/ml) for 10 minutes, washed, and labelled with [^{14}C]Gal (open circles in A). Cells were resuspended in the presence of HRP (1 mg/ml) for 60 minutes at 37°C. After cooling on ice, cells were washed free from external HRP, prior to labelling with [^{3}H]Gal (closed circles in A). Cells were resuspended in the absence of HRP and at t=0 (before warming) and at indicated times at 37°C, samples were taken by cooling on ice. Samples were treated with ß-galactosidase (0,2 U/ml for 30 minutes on ice) to release cell-surface label as shown in A. The samples for each time point were then treated with DAB in the presence (closed symbols in B and C) or absence of H_2O_2 (open symbols in B and C), followed by resuspension in detergent (1% Triton X-100) and homogenisation in a cell cracker (cf. Methods). Detergent solubility was measured as the fraction of the total label remaining in the supernatant after centrifugation on a 35% wt/wt sucrose cushion for 60 minutes at 10^{5}xg (cf. Methods). Radioactivity was measured after complete separation of isotopes as $^{3}H_2O$ and $^{14}CO_2$. Squares and circles in B and C refer to independent experiments. B: ^{3}H-labelled membrane marker. C: ^{14}C-labelled membrane marker.

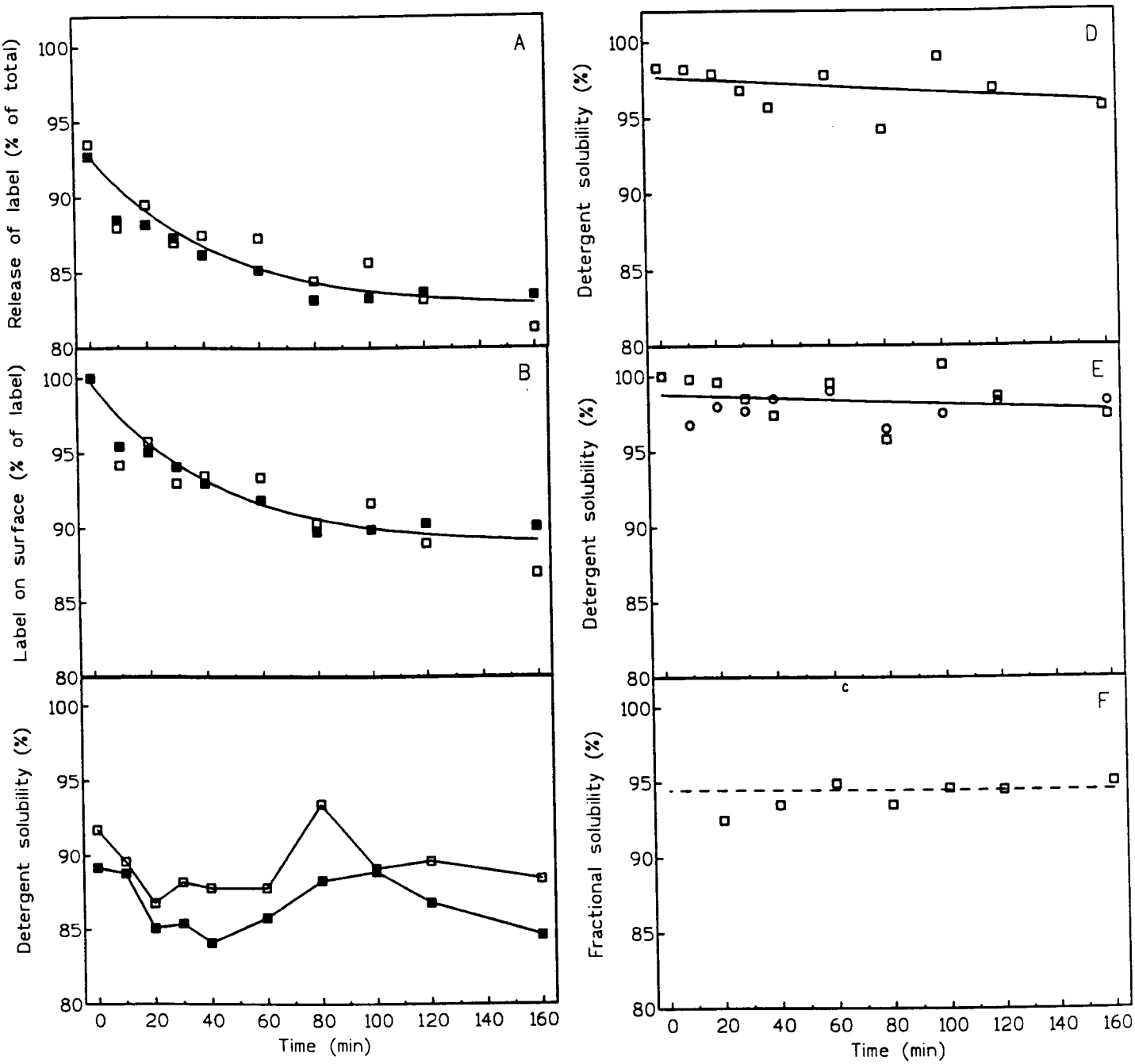
A
B
C
D
E
F
Release of label (% of total)
Label on surface (% of label)
Detergent solubility (%)
Fractional solubility (%)
Time (min)
100
95
90
85
80
0
20
40
60
80
100
120
140
160

FIG. 3.7

Fig. 3.7: Endocytic uptake of HRP at 37°C, followed immediately by internalisation of plasma membrane glycoconjugates at 16°C. A cell suspension was divided into two equal portions and incubated in the presence (closed symbols) or absence (open symbols, except in D and E) of HRP (1 mg/ml) for 30 minutes at 37°C. Cells were cooled and washed free from HRP. Cells were pretreated with ß-galactosidase (0.1 U/ml) for 10 minutes, washed and labelled with [^{3}H]Gal (closed symbols) or [^{14}C]Gal (open symbols, except in D and E) respectively. Cells were combined and resuspended in the absence of HRP. At t=0 (before warming) and at the indicated times at 16°C, samples were taken by cooling on ice. Cells were treated with ß-galactosidase (0.2 U/ml for 30 minutes on ice) to release cell-surface label as shown in A, and to determine the degree of internalization as shown in B (The fraction of label that could be released from cells without internalisation after labelling, i.e. values at t=0 in A, was normalised to represent 100% of label on the cell surface and all other values were normalised accordingly). The samples for each time point were then treated with DAB/H_2O_2 followed by resuspension in detergent (1% Triton X-100). Detergent solubility was measured as the fraction of the total label remaining in the supernatant after centrifuging at 10^5xg (cf. Methods). Radioactivity was measured after complete separation of isotopes as $^{3}H_2O$ and $^{14}CO_2$. Solubility values for the ^{3}H-label (closed symbols in C) were corrected for intra-experimental variation by dividing with the corresponding solubility values as measured for the ^{14}C-label (internal negative controls, open symbols in C), as shown in D. The ^{3}H/^{14}C solubility ratios for t=0 samples were taken as indicating 100% solubility (t=0 in D) and all other ratios (for t>0 within the same experiment) were normalised accordingly, as in E. Squares and circles refer to independent experiments. The fractional solubility was calculated from the data in A and D, as shown in F. Round symbols in E show additional data from an independent experiment.

alternative kinetics as proposed for scenario of type A (Fig. 1.4), these results indicated that HRP, as endocytic contents marker, was processed in a sequential manner.

The two different labels which were available as membrane marker, viz. [^{3}H]Gal and [^{14}C]Gal, made it possible to study two different kinetic scenarios in one experiment. Using [^{14}C]Gal in the steady-state distribution for analysing the processing of HRP during a chase along the endocytic pathway towards lysosomes (as above, cf. scenario type A, Fig. 1.4), the processing of membrane could be studied simultaneously, in the identical cells, by labelling the cell surface with [^{3}H]Gal to be internalized after the HRP pulse (cf. section 3.3 above, and scenario type B, Fig. 1.5). This approach, however, left no label for use as an internal negative control.

As shown in Fig. 3.6A, the ^{14}C-labelled membrane marker was at steady-state, while the other (^{3}H-labelled) became internalised by first-order kinetics. While HRP was chased along the endocytic pathway, the solubility of the steady-state marker (^{14}C) gradually increased, indicative of the sequential processing of HRP in endosome (Fig. 3.6C). Simultaneously, the ^{3}H-labelled membrane marker, being internalized after the HRP pulse, became susceptible to crosslinking, which showed that the membrane marker was catching up with the sequentially processed contents marker (Fig. 3.6B). Obviously, the data in Fig. 3.6 were not as accurate as in previous experiments, since no internal negative control was available to correct for

experimental inaccuracies (variation as indicated by using the omission of H_2O_2 for negative controls). Nevertheless, the crude data are compatible with the results of the corresponding experiments where internal negative controls were available (cf. Fig. 3.3 and 3.5).

3.6 Effect of low temperature on endosome processing

To determine the effect of low temperature on crosslinking by DAB reaction, the same endocytosis protocol was followed as in Section 3.3. The membrane marker was internalised at 16°C (unlike 37°C as was done previously) for increasing times into the endocytic pathway in the presence of HRP (or without HRP for negative controls) (Fig. 3.7).

As the membrane flow at 16°C is about 10 fold lower than at 37°C, a larger time scale was therefore necessary for comparative studies. Selective removal of cell surface label to measure the degree of internalisation was achieved by treating cells with glycosidases. As shown in Fig. 3.7A, glycosidase treatment removed about 93% of the label when this was all on the cell surface (at t=0, prior to membrane label internalisation). This value was used to represent 100% of the label on the cell surface and all values for the later time points were normalised accordingly. As shown in Fig. 3.7B, about 12% of label was redistributed to intracellular membranes after 2½ hours.

As shown in Fig. 3.7C, the values for membrane solubility were very similar to those of the negative controls. The overall degree of crosslinking after 2½ hours of endocytosis was only about 3% (Figs. 3.7D and 3.7E), and the fractional solubility (Fig. 3.7F) was constant at about 95% throughout the time course.

When the temperature was raised from 16°C to 37°C after two hours of chase, there was about 5% increase in the steady-state distribution of label to about 16% label on intracellular membranes over the next 5 minutes, but still no change occurred with respect to the degree of detergent solubility of the membrane bound marker (unpublished results).

CHAPTER 4

DISCUSSION AND CONCLUSION

In this study, the nature of the endosome compartment, with respect to its sorting function, was investigated. In the sequential model, the endosome is perceived as a time-structured compartment, through which membrane and contents move in a sequential manner, without mixing (Fig. 1.3A). In the random model, internalised membrane and contents are pooled, randomised, followed by transfer and recycling based on chance.

Firstly, when membrane marker was internalised for increasing times into the endocytic pathway in the presence of HRP according to experimental protocol represented by scenario of type C (Fig. 1.6), the result indicated random processing of membrane marker in endosomes (Fig. 3.2). The data obtained from experiments performed according to scenario type B (Fig. 1.5) also suggested intermingling of newly internalised membrane marker with previously endocytosed HRP (Fig. 3.3). A plot of these data in terms of "fractional solubility" (Fig. 3.3D), i.e. considering only the solubility of intracellular label, clearly shows that newly internalised label experienced the same extent of colocalisation with HRP as was the case for the steady-state membrane marker in endosomes.

These results contradict those reported by Ajioka & Kaplan (35), where, on HeLa cells, membrane bound receptors for transferrin seem to move through the endosome in a sequential manner. Those

experiments were, however, performed at 28°C in order to slow down the endocytic process and obtain a better resolution in time. At 16°C, the present system also displayed sequential rather than random processing of endocytic membrane marker. Although the accumulation of cell-surface membrane marker in intracellular compartments at 16°C occurs with first-order kinetics as at 37°C, the fractional solubility of membrane marker, Fig. 3.7F, remained at about 95% over more than 2 hours. At low temperatures, newly internalised label does not colocalise with vesicles containing previously loaded HRP as is the case at 37°C (Fig. 3.3). This is reminiscent of <u>in vivo</u> observations where the endosome has been seen as a continuous tubular network at 37°C but which breaks down into smaller organellar fragments upon cooling to 20°C (14).

Secondly, when experiments were performed according to scenario of type A (Fig. 1.4: chasing HRP in or out of steady-state membrane marker) the time course by which HRP, as contents marker, proceeded along the endocytic pathway suggested that it was moving along to the lysosomes in a sequential manner (Figs. 3.4 & 3.5). The curves as indicated (Figs. 3.4 C,E & 3.5 C,D), are as for first-order kinetics. The question arises as to what mechanism could account for such a steady-state distribution. An obvious explanation would be that there is a constant probability of recycling throughout the pathway. In such a case, while membrane marker enters along the pathway, the amount of label remaining (not yet recycled at a particular stage) will decline exponentially with distance. Such a mechanism could be

postulated in view of endosomes operating as an interconnected tubular network (14,22). Another explanation for the exponential behaviour could be that segregation of contents (HRP, or HRP-free medium) from membrane marker is based on a randomly occurring slowest step. Such a step could be the random encounter between endocytic carrier vesicles (18,32) and lysosomes in the perinuclear region for delivery of contents and simultaneous recycling of membrane marker. Random movement of endocytic vesicles towards the perinuclear region has indeed been observed (42). As such, it would be a very attractive mechanism to explain the presently observed exponential time course (Figs. 3.4 C,E and 3.5 C,D). When interpreted in terms of sequential movement of HRP along the endocytic pathway, the curves reflect the steady-state distribution of cell surface-derived membrane marker along this pathway.

So far, this distribution is not known, and as suggested here, may not be linear: Membrane marker, which was at steady state along the endocytic pathway, became associated with (during uptake) or liberated from (during chase HRP by the time course indicated (Figs. 3.4 and 3.5). When assuming that HRP moved at a constant rate throughout the pathway, these time courses would reflect the steady-state distribution of the membrane marker.

Whereas the first of the two explanations above would require strict sequential movement of contents, the latter would also be compatible with limited intermingling of contents. Such intermingling at later, prelysosomal stages of the endocytic

pathway have been reported, where in fibroblast cells endocytic contents appeared to become mixed after sequential uptake (36).

Segregation between membrane marker and contents (HRP) has been defined operationally as membrane marker escaping from being trapped by DAB-crosslinking when no longer colocalizing with sufficient HRP. With membrane recycling occurring by vesicular budding off endocytic organelles which contain HRP (43), the question arises whether recycling vesicles would not contain enough HRP to maintain sufficient trapping of memberane marker. This can be expected if bulk segregation of endocytic contents (volume) from membrane (surface area) is governed only by the increased surface/volume ratio of the smaller recycling vesicles (cf. 44). Morphological evidence suggests that membrane marker on recycling vesicles may indeed escape trapping by DAB-crosslinking: The tubular parts of endosomes in macrophages, from where recycling occurs, do not stain for DAB reaction-product after HRP uptake via fluid-phase endocytosis, but only when HRP has been taken up via the mannose receptor (45); In L-cells, HRP-mediated staining of recycling vesicles cannot be observed during early stages (<39 min) of HRP uptake, but only after HRP has accumulated in lysosomes (43). In the present system of $P388D_1$ macrophage-like cells, HRP release by retro-endocytosis is less than 1% of the uptake rate (data not shown; cf. 46).

In conclusion, the major finding in this study is that in macrophage cells, $P388D_1$, the contents marker, HRP, is processed

in a sequential manner as against membrane marker, which is processed in a random fashion. The structural requirements of endosomes which would allow for this difference between the processing of membrane vs. contents marker could be a continuous endosomal tubular network as was recently observed for live cells (14). This network broke down at low temperature, and again, would explain the present observation of membrane marker no longer being processed in a random manner at 16°C.

As a follow-up to this study and for comparative purposes, other cell types, for instance HeLa cells or fibroblasts, may be investigated with the same experimental protocols and markers used in this study.

REFERENCES

1. Steinman, R.M., J.M. Silver, and Z.A. Cohn. 1974. Pinocytosis in fibroblasts: Quantitative studies in vitro. J. Cell Biol. 63: 949-969.

2. Steinman, R.M., S.E. Brodie, and Z.A. Cohn. 1976. Membrane flow during pinocytosis: A stereological analysis. J. Cell Biol. 68: 665-687.

3. Steinman, R.M., I.S. Mellman, W.A. Muller, and Z.A. Cohn. 1983. Endocytosis and recycling of plasma membrane. J. Cell Biol. 96: 1-27.

3a. Oka, J.A., M.D. Christensen, and P.H. Weigel. 1989. Hyperosmolarity inhibits galactosyl receptor-mediated but not fluid phase endocytosis in isolated rat hepatocytes. J. Biol. Chem. 264: 12016-12024.

4. Stahl, P., P.H. Schlesinger, E. Sigardson, J.S. Rodman, and Y.C. Lee. 1980. Receptor-mediated pinocytosis of mannose glycoconjugates by macrophages: characterisation and evidence for receptor recycling. Cell 19: 207-215.

5. Aebi, U., W.E. Flower, G. Isenberg, T.D. Pollard, and P.R. Smith. 1981. Crystalline actin sheets: Their structure and polymorphism. J. Cell Biol. 91: 340-351.

6. Porter, K.R. 1984. Cytomatrix: A short history of its study. J. Cell Biol. 99: 3(s)-12(s).

7. Sheterline, P. 1983. Drugs affecting contractile systems. In: Mechanisms of cell motility and molecular aspects of contractility. pp. 167-176.

8. Goldstein, J.L., R.G.W. Anderson, and M.S. Brown. 1979. Coated pits, coated vesicles and receptor-mediated endocytosis. Nature 279: 679-685.

9. Brodsky, F.M. 1988. Living with clathrin: its role in intracellular membrane traffic. Science 242: 1396-1402.

10. Maezawa, S., T. Yoshimura. 1990. Determination of the regions of the clathrin molecule inducing membrane fusion. Biochem. 29: 1813-1817.

11. Mueller, S.C., and A.L. Hubbard. 1986. Receptor-mediated endocytosis of asialoglycoproteins by rat hepatocytes. J. Cell Biol. 102: 932-942.

12. Casey K.A., K.M. Maurey, and B. Storrie. 1986. Characterization of early compartments in fluid phase pinocytosis: a cell fractionation study. J. Cell Sci. 83: 119-133.

13. Schmid, S.L., R. Fuchs, P. Male, and I. Mellman. 1988. Two distinct subpopulations of endosomes involved in membrane recycling and transport to lysosomes. Cell 52: 73-83.

14. Hopkins, C.R., A. Gibson, M. Shipman, and K. Miller. 1990. Movement of internalised ligand-receptor complexes along a continuous reticulum. Nature 346: 335-338.

15. Galloway, C.J., G.E. Dean, M. Marsh, G. Rudnick, and I. Mellman. 1983. Acidification of macrophage and fibroblast endocytic vesicles in vitro. Proc. Natl. Acad. Sci. USA 80: 3334-3338.

16. Cain, C.C., R. Murphy. 1988. A chloroquine-resistant Swiss 3T3 cell line with a defect in late endocytic acidification. J. Cell Biol. 106: 269-277.

17. Beaumelle, B.D., and C.R. Hopkins. 1989. High yield of functionally competent endosomes from mouse lymphocytes. Biochem. J. 264: 137-149.

18. Gruenberg, J., G. Griffiths, and K.E. Howell. 1989. Characterisation of the early endosome and putative endocytic carrier vesicles in vivo and with an assay of vesicle fusion in vitro. J. Cell Biol. 108: 1301-1316.

19. Gruenberg, J., and K.E. Howell. 1988. Cell-free Analysis of Membrane Traffic, Alan R. Liss Inc., pp. 317-331.

20. Gruenberg, J., and K.E. Howell. 1987. An internalised transmembrane protein resides in a fusion-competent endosome for less than 5 minutes. Proc. Natl. Acad. Sci. USA 84: 5758-5762.

21. Ward, D.M., D.P. Hachenyos, and J. Kaplan. 1990. Fusion of sequentially internalised vesicles in alveolar macrophages. J. Cell Biol. 110: 1013-1022.

22. Warren, G. 1990. Trawling of receptors. Nature 346: 318-319.

22a. Holtzman, E. 1989. Lysosomes, in "Cellular Organelles" Series, Plenum Press, London.

23. Ferris, A.L., J.C. Brown, R.D. Park, and B. Storrie. 1987. Chinese hamster ovary cell lysosomes rapidly exchange contents. J. Cell Biol. 105: 2703-2712.

24. Haylett, T., and L. Thilo. 1986. Limited and selective transfer of plasma membrane glycoproteins to membrane of secondary lysosomes. J. Cell Biol. 103: 1249-1256.

25. Farquhar, M.G. 1985. Progress in unravelling pathways of Golgi traffic. Ann. Rev. Cell Biol. 1: 447-488.

26. Dahms, N.M., P. Lobel, and S. Kornfield. 1989. Mannose-6-phosphate receptors and lysosomal enzyme targeting. J. Biol. Chem. 264: 12115-12118.

27. Gonzalez-Noriega, A., R. Coutiño, V.M. Saaverda, and R. Barrera. 1989. Adsorptive endocytosis of lysosomal enzymes by human fibroblasts: Presence of two different functional systems that deliver an acid hydrolase to lysosomes. Arch. Biochem. & Biophys. 268: 649-658.

28. Griffiths, G., B. Hoflack, K. Simons, I. Mellman, and S. Kornfield. 1988. Mannose-6-phopshate receptor and the biogenesis of lysosomes. Cell 52: 319-341.

29. Thilo. L. 1985. Selective internalization of granule membrane after secretion in mast cells. Proc. Natl. Acad. Sci. USA 82: 1171-1715.

30. Reichner, J.S., S.W. Whiteheart, and G.W. Hart. 1988. Intracellular trafficking of cell surface sialoglycoconjugates. J. Biol. Chem. 263: 16316-16326.

31. Jin, M., G.G. Sahagian, and M.D. Snider. 1989. Transport of surface mannose-6-phosphate receptor to the Golgi complex in cultured human cells. J. Biol. Chem. 264: 7675-7680.

31a. Roederer, M., R. Bowser, and R.F. Murphy. 1987. Evidence for a maturation model for the formation of lysosomes. J. Cell. Physiol. 131: 200-209.

32. Griffiths, G., and J. Gruenberg. 1991. The arguments for pre-existing early and late endosomes. Trends in Cell Biology 1: 5-9.

33. Storrie, B., P.R. Robert, M. Sachdeva, K.M. Maurey, and C. Oliver. 1984. Evidence for both pre-lysosomal and lysosomal intermediates in endocytic pathways. J. Cell Biol. 98: 108-115.

34. Stoorvogel, W., G.J. Strous, H.J. Geuze, V. Oorschot, and A.L. Schwartz. 1991. Late endosomes derive from early endosomes by maturation. Cell 65: 417-427.

35. Ajioka, R.S., and J. Kaplan. 1986. Intracellular pools of transferrin receptors result from constitutive internalization of unoccupied receptors. Proc. Natl. Acad. Sci. USA 83: 6445-6449.

36. Salzman N.H., and F.R. Maxfield. 1988. Intracellular fusion of sequentially formed endocytic compartments. J. Cell Biol. 106: 1083-1091.

37. Ajioka, R.S., and J. Kaplan. 1987. Characterization of endocytic compartments using the Horseradish Peroxidase-

Diaminobenzidine density shift Technique. J. Cell Biol. 104: 77-85.

38. Thilo, L. 1985. Methods in Enzymology 98: 415-421.

39. Courtoy, P.M., J. Quintart, and P. Baudhuin. 1984. Shift of equilibrium density induced by 3,3'-diaminobenzidine cytochemistry: A new procedure for the analysis and purification of peroxidase-containing organelles. J. Cell Biol. 98: 870-876.

40. Smith, J.P., M.H. Friede, B.J. Scott, and C. von Holt. 1988. Isolation of nuclei from mellitin-destabilised cells. Anal. Biochem. 169: 390-394.

41. Cook, J.A., and J.B. Mitchell. 1989. Viability measurements in mammalian cell systems. Anal. Biochem. 179: 1-7.

42. De Brabander, M., R. Nuydens, H. Geerts, and C.R. Hopkins. 1988. Dynamic behavior of the transferrin receptor followed in living epidermoid carcinoma (A431) cells with nanovid microscopy. Cell Motil. Cytoskel. 9: 30-47.

43. Van Deurs, B., and K. Nilausen. 1982. Pinocytosis in mouse L-fibroblasts: Ultrastructural evidence for a direct membrane shuttle between the plasma membrane and the lysosomal compartment. J. Cell Biol. 94: 279-286.

44. Dunn, K.W., T.E. McGraw, and F.R. Maxfield. 1989. Iterative fractionation of recycling receptors from lysosomally destined ligands in an early sorting endosome. J. Cell Biol. 109: 3303-3314.

45. De Chastellier, C., T. Lang, A. Ryter, and L. Thilo. 1987. Exchange kinetics and composition of endocytic membranes in terms of plasma membrane constituents: a morphometric study. Eur. T. Cell Biol. 44: 112-123.

46. McKinley, D.N., and H.S. Wiley. 1988. Reassessment of fluid-phase endocytosis and diacytosis in monolayer cultures of human fibroblasts. J. Cell. Physiol. 136: 389-397.